URBAN BUILDING ENERGY MODELING: INTEGRATING DYNAMIC AND DATA-DRIVEN MODELS FOR TIME-SERIES ANALYSIS

A Thesis

by

Said Bolluk

Submitted to the
Graduate School of Sciences and Engineering
in Partial Fulfillment of the Requirements for
the Degree of

Master of Science

in the
Department of Civil Engineering

Özyeğin University
January 2024

URBAN BUILDING ENERGY MODELING: INTEGRATING DYNAMIC AND DATA-DRIVEN MODELS FOR TIME-SERIES ANALYSIS

Approved by:

Asst. Prof. Senem Seyis
Dept. of Civil Engineering
Özyeğin University

Asst. Prof. Reyhan Aydoğan
Dept. of Computer Science
Özyeğin University

Asst. Prof. Gözde Gali Taşçı
Dept. of Interior Architecture
Beykent University

Date Approved: January 5, 2024

To my dear family...

ABSTRACT

This study addresses a critical gap in Urban Building Energy Modeling (UBEM) by introducing an innovative hybrid approach that combines dynamic and statistical models. Previous hybrid studies faced challenges in result validation, model calibration, and delivering predictions at high temporal resolution. To fill this gap, the study presents an integrated UBEM for time-series analysis. The methodology involves creating a dynamic model for 13 buildings on a university campus, with key parameters calibrated using Bayesian Optimization. This calibration reduces the simulation's annual Mean Absolute Percentage Error (MAPE) from 21.56% to 4.60% and the monthly MAPE from 22.14% to 9.90%. The calibrated dynamic model's hourly energy consumption data is then incorporated into a statistical model, a Long Short-Term Memory (LSTM) network utilized in time-series regression. The statistical model predicts the hourly energy consumption with an average R-squared value of 0.915.

The proposed hybrid model facilitates the creation of synthetic hourly energy consumption data for urban building stocks. In this sense, the energy use patterns derived from the hourly consumption can be combined with the building characteristics to identify parameters that shape the building energy demand. The hybrid model can also optimize the building energy efficiency design by exploring various configurations in the building envelope and operational schedules and minimizing the energy consumption and the resultant environmental impact. When adapted to the urban scale, this hybrid model can provide valuable insights for urban planners in identifying high-demand areas and implementing energy-efficient interventions based on high-resolution temporal energy consumption data. Instead of testing energy and

cost-efficiency scenarios using dynamic simulations, the proposed hybrid model can effectively monitor and control the hourly building energy use over time-series analysis once calibrated.

This study underscores the potential of hybrid modeling in UBEM despite facing challenges, like complexities in generating the validation data from a limited number of metered energy consumption and computational constraints. In summary, this research introduces a robust hybrid UBEM and draws a roadmap for future research to comprehend urban building energy demand accurately. Future research includes reliability improvements for the validation and input data, efficient and precise dynamic modeling approaches, and utilizing thermal interactions between buildings within the statistical model.

ÖZETÇE

Bu çalışma, dinamik ve istatistiksel modelleri birleştiren yenilikçi bir hibrit yaklaşım sunarak Kentsel Bina Enerji Modellemesindeki (UBEM) kritik bir boşluğu dikkat çekmektedir. Önceki hibrit çalışmalar, sonuçların doğrulanması, model kalibrasyonu ve tahminlerin yüksek zamansal çözünürlükte sunulması konularında zorluklarla karşılaşıyordu. Bahsi geçen sorunlara çözüm üretmek amacıyla bu çalışma, istatiksel ve dinamik modelleri bütünleştiren bir hibrit model sunmaktadır. Bu kapsamda ilk olarak 13 binalık bir üniversite kampüsünün dinamik modeli oluşturulmuş, daha sonra bu modelin temel parametreleri Bayes Optimizasyonu kullanılarak kalibre edilmiştir. Kalibrasyon sonucunda dinamik model simülasyonunun yıllık Ortalama Mutlak Yüzde Hatası (MAPE) %21,56'dan %4,60'a ve aylık %22,14'ten %9,90'a düşmüştür. Kalibre edilen dinamik model daha sonra saatlik enerji tüketim verileri yaratmada kullanılmıştır. Bu tüketim verileri, çalışmanın bir diğer kısmı olan istatiksel modelin doğrulama verilerini teşkil etmektedir. İstatiksel modelde her bir bina için bir tür Özyinelemeli Sinir Ağı (RNN) olan Uzun Kısa Süreli Bellek (LSTM) modeli oluşturulmuş, daha sonra bu modeller zaman serisi regresyon analiziyle binaların saatlik enerji tüketimlerini tahmin etmede kullanılmıştır. Regresyon sonuçlarına göre modellerin ortalama determinasyon katsayısı (R-sqaured) 0.915'tir.

Önerilen hibrit model, kentsel bina stokları için sentetik saatlik enerji tüketimi verilerinin oluşturulmasını kolaylaştırmaktadır. Bu anlamda, saatlik tüketimlerden elde edilen enerji kullanım davranışları, binaların enerji talebini şekillendiren parametreleri belirlemek için binaların ayırt edici özellikleriyle birleştirilebilir (ör. yalıtım bilgileri) . Hibrit model aynı zamanda bina kabuğundaki ve operasyonel programlardaki çeşitli konfigürasyonları keşfederek enerji tüketimini ve bunun sonucunda ortaya

çıkan çevresel etkiyi en aza indirebilir. Bu sayede önerilen hibrit model enerji verimli bina tasarımında değerlendirilebilir. Saatlik çözünürlükteki bina enerji tüketimi verilerini tahmin edebilen bu hibrit model, kentsel ölçeğe uyarlandığında kent planlayıcılarına yüksek enerji tüketen bölgelerin belirlenmesi ve bu bölgeler için gerekli önlemlerin alınması konusunda değerli bilgiler sağlayabilir. Önerilen hibrit model, dinamik simülasyonlar üzerinden enerji ve maliyet verimliliği senaryolarını test etmek yerine, istatiksel modelin sunduğu zaman serisi analizi yöntemiyle saatlik bina enerji kullanımını etkili bir biçimde tahmin edebilir ve kontrol edebilir.

Bu çalışmada, doğrulama verileri oluşturulurken ölçülmüş tüketim verisine sahip ay sayısının az olması ve simülasyon ve tahminlerin yoğun hesaplama gücüne ve uzun bir zamana ihtiyaç duyması gibi sorunlarla karşılaşılmıştır. Fakat tüm zorluklara rağmen bu çalışma, UBEM alanındaki hibrit modellerin potansiyeline dikkat çekmiştir. Özetle, bu araştırma güçlü bir hibrit UBEM'i tanıtırken kentsel bina enerji talebini doğru şekilde anlamak için gelecekteki araştırmalara bir yol haritası çizmektedir. Gelecekteki yürütülmesi planlanan araştırmalar arasında doğrulama ve girdi verilerinin güvenilirliğinin iyileştirilmesi, verimli ve tutarlı dinamik modelleme yöntemlerinin geliştirilmesi ve binalar arasındaki termal etkileşimi göz önüne alan parametrelerin istatiksel modele tanıtılması yer almaktadır.

ACKNOWLEDGEMENTS

I extend my deepest gratitude to my advisor, Assistant Professor Senem Seyis, whose guidance, wisdom, and unwavering support have been instrumental throughout this thesis journey. I am also profoundly thankful for the invaluable contributions of Assistant Professor Reyhan Aydoğan and Assistant Professor Ece Kalaycıoğlu Özdemir, whose insights and encouragement significantly enriched the development of my research.

My sincere appreciation goes to my family and friends for their constant support, understanding, and encouragement during this challenging yet rewarding academic effort.

I want to thank Zachary Michael Berzolla for generously providing expertise and support to elevate the use of UMI. Also, special thanks must go to the Scientific and Technological Research Council of Türkiye (TÜBİTAK) for their support through the 3501 - Career Development Program. This research, which is part of a TÜBİTAK project titled "Kentsel Bina Enerji Modellemesi İçin Hibrit Yaklaşim Geliştirilmesi" and identified by the reference number "222M488", was made possible by their generous assistance.

TABLE OF CONTENTS

LIST OF TABLES

LIST OF FIGURES

CHAPTER I

INTRODUCTION

Building energy demand increased by 60 million tons globally in 2022, which constitutes more than 19% of the increase in greenhouse gas emissions from the world's overall energy consumption [3]. The construction industry should be investigated thoroughly to understand and reduce such a vast energy use. The occupant-related uncertainties [4] and the diversity in the characteristics of the urban building stocks [5] complicate the analysis of the building energy demand with reliable assumptions. Similarly, the construction industry's partial failure in digitalization and the resulting lack of comprehensive data hinder studies examining the energy consumption of urban building stocks [6] [7]. However, well-equipped urban building energy models can provide sustainable solutions to monitor and control urban building energy use [8] [9]. Different modeling approaches have been introduced to the literature in recent years to overcome these problems. In this sense, Swan and Ugursal classified these approaches into two types: top-down and bottom-up approaches [10]. The top-down approach relies on historical data to make predictions. It examines the overall energy consumption of urban building stocks to create long-term plans that consider urban planning and economic and technological growth strategies in cities. Since the goal is to understand general trends, the input data for top-down models can be broad. This can include basic information for a district, like demographics (e.g., household income or employment rate), climate conditions, and general statistics from the construction industry (e.g., rental prices and construction costs) [10].

On the other hand, the bottom-up approach focuses on understanding the factors influencing the energy consumption of urban building stocks [10]. Its goal is to develop energy reduction strategies for individual buildings or groups of buildings at the urban level. This method demands in-depth insights into regional climatic conditions and the characteristics of the buildings and occupants within the chosen district. Bottom-up urban building energy models can identify potential energy savings through retrofitting strategies across building, occupant, and grid components [11]. The strengths and weaknesses of these models may cause uncertainty in choosing the most appropriate model for an urban-level study. For example, statistical bottom-up models use machine learning algorithms based on historical data to predict building energy consumption. However, statistical bottom-up models might ignore thermal interaction between buildings. In addition, statistical models might be insufficient to accurately predict energy consumption at higher resolutions (e.g., hourly consumption) as it is challenging to include time-dependent variables in these models, such as climate data (e.g., temperature) and building operational schedules (e.g., heating schedule) [12]. On the other hand, dynamic bottom-up models utilizing computational fluid dynamics or more simplified methods [13] may require many resources in terms of computation and time when performing realistic energy simulations [14]. The typical approach in urban building energy modeling (UBEM) is to choose a bottom-up single model suitable for the study's purpose and scope [15]. Although there are studies providing a hybrid approach by utilizing dynamic and statistical models, these current studies either lack parameter calibration [16] and model validation [17], provide predictions at a low temporal resolution [18], or do not utilize a proper dynamic model [19]. Thus, there is a need for a novel hybrid approach in UBEM.

This study addresses the limitations identified in previous research on UBEMs by proposing a novel approach that integrates powerful elements of statistical and dynamic models. Inspecting the hourly energy consumption of buildings is essential to develop energy reduction strategies for urban building stocks. Statistical models struggle to predict hourly energy use accurately. Dynamic models can fix this problem but are complex and need detailed data and time. Hence, there is a need for an integrated approach. In this sense, a dynamic model of campus buildings is created, and its essential parameters that affect the building energy consumption most are calibrated using Bayesian Optimization. This calibrated model generates consistent synthetic hourly energy consumption data, which is then used to validate the statistical models. Finally, the statistical model conducts a time-series analysis to predict the hourly energy consumption of the buildings.

The proposed hybrid model in this study contributes to optimizing energy-efficient building design. Through testing various scenarios for building insulation and operational schedules, this hybrid model provides actionable insights to reduce energy consumption. Instead of analyzing the effect of each scenario over the dynamic model, once tuned, the hybrid model can effectively predict the resultant energy savings using time-series analysis. It also offers the capability to anticipate and mitigate the impact of climate change thanks to the effective use of weather data. Moreover, hourly synthetic energy consumption data enable an understanding of the deviations in the building energy consumption patterns. When these patterns are combined with the building characteristics, the proposed hybrid model can extract the determinant parameters shaping the building energy demand. When adapted to the urban context, this hybrid model can provide valuable insights for urban planners to identify high-demand areas and implement energy-efficient interventions based on high-resolution temporal energy consumption data. The workflow of the proposed methodology is illustrated in Figure 1. In the following chapters, the related UBEM studies will be summarized, the details of creating the dynamic and statistical models will be presented, and the contributions and limitations of the study will be discussed.

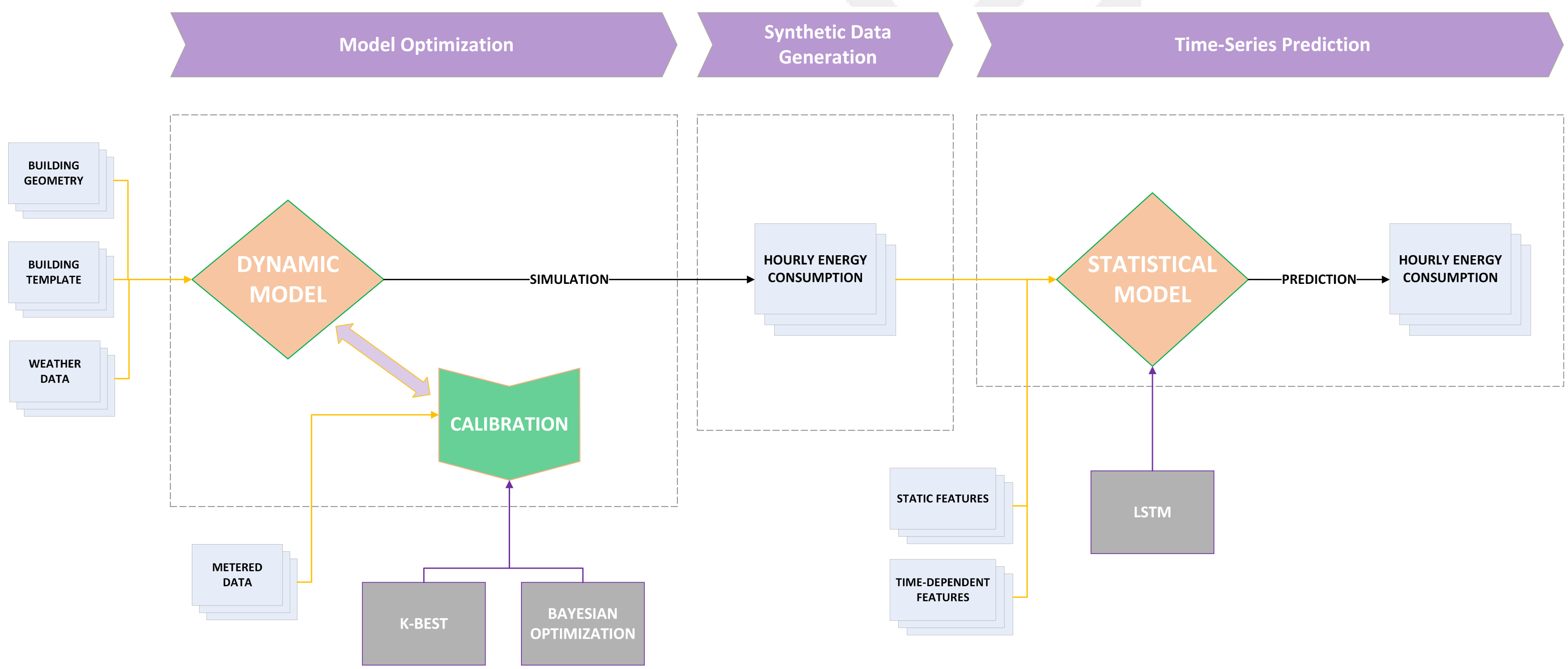

Figure 1 : Methodology Workflow

CHAPTER II

RESEARCH BACKGROUND

This section comprises essential insights into the methodologies employed in this study. It provides an overview of the simulation tools, machine learning models, their associated evaluation metrics, and the optimization algorithm used for analysis.

2.1 Urban Modeling Interface (UMI)

The Urban Modeling Interface (UMI) is a simulation tool the MIT Sustainable Design Lab developed [1]. UMI is integrated into a computer-aided design (CAD) program called Rhinoceros 3D (Rhino) that provides a user-friendly environment for the modeling and simulation steps [20]. UMI was designed to explore the impact of buildings on urban environments, covering a series of analyses, such as operational and embodied energy use, neighborhood walkability, daylighting, food production, and district-level energy supply. UMI employs a simplified modeling approach known as Ideal Loads Air System by EnergyPlus [21] for energy simulations. Creating an Urban Building Energy Model (UBEM) through UMI requires three primary input parameters: (1) building geometries, (2) building templates, and (3) weather data.

Building geometries in the UBEM are derived from building footprints available through mapping services or GIS software. UMI extrudes these footprints, assigning volume to each building based on its height. The various surfaces of a building, identified by their normal vectors' orientation (upward for roofs, downward for ground surfaces, and others for facades), are used to create multiple zones for detailed energy simulation. This process, known as automatic zoning [22], involves separating buildings by floors and establishing core and perimeter zones for each floor. UMI operates the Shoeboxer algorithm to create thermal zones, utilizing solar radiation maps from local weather data to divide building facades into bins. This captures sunlight exposure variations and allows for a comprehensive analysis of how different building parts are impacted by solar radiation throughout the day and across seasons. The Shoeboxer algorithm clusters these bins into groups with similar orientation and solar exposure. The initialization of cluster centers is done randomly. This introduces a stochastic element where the cluster number and characteristics may vary. Each resulting cluster forms a thermal zone, and they are visually represented as a shoebox object (Figure 2).

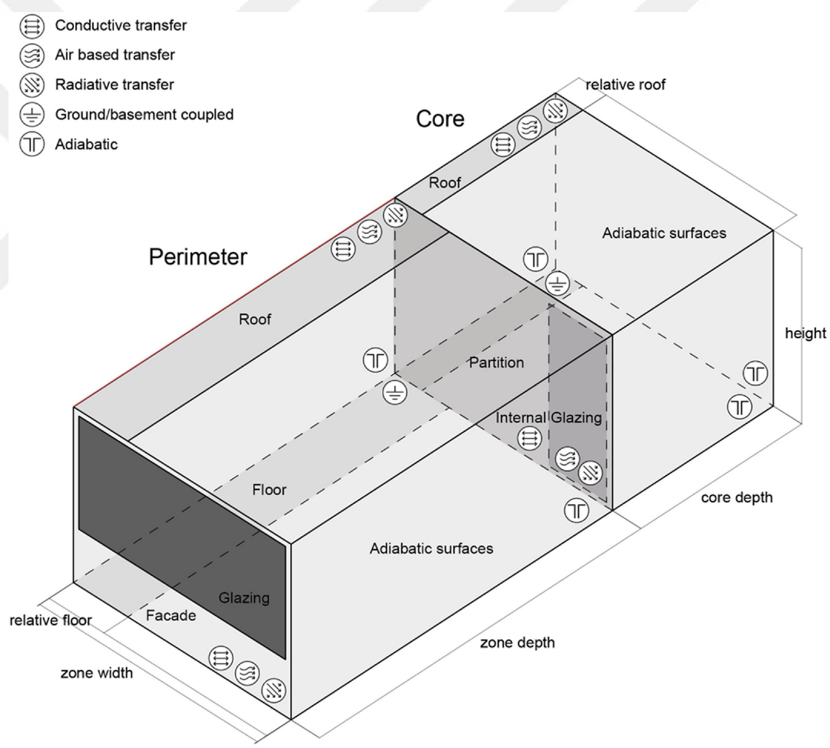

Figure 2 : Shoebox geometry and heat transfer setup per surface. Retrieved from [1]

Once the shoebox objects are determined, UMI performs the energy simulation, where it designates one building as the target and identifies surrounding buildings as shading objects. To perform this simulation effectively, UMI relies on more than just building geometry. A building template defines a building's energy consumption characteristics, containing materials, construction setups, and details for various components such as floors, interior partitions, facades, roofs, and ground-facing elements. Information about glazing properties, blinds, shading systems, operational schedules (e.g., occupant numbers, equipment, lighting power densities), and HVAC properties are also included. This template is formatted in JavaScript Object Notation (JSON) and can be edited using text editors or the UMI Template Editor plug-in (Figure 3).

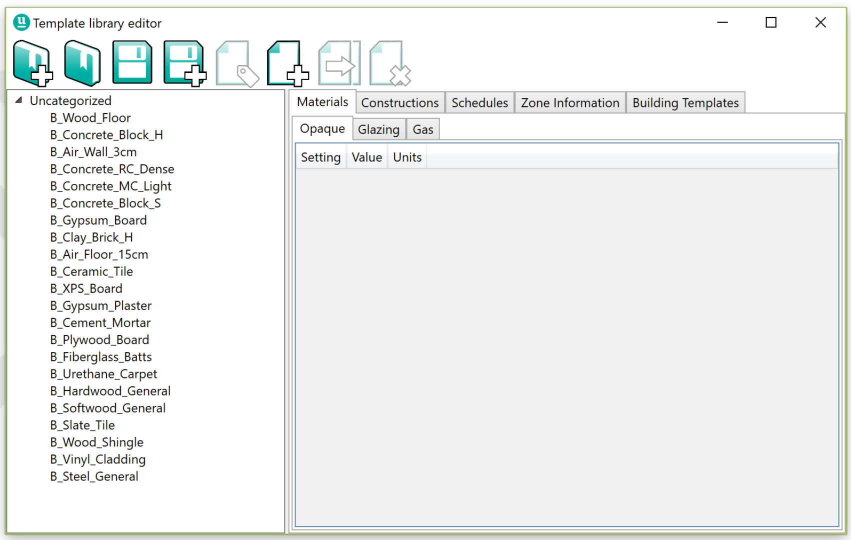

Figure 3 : UMI Template Editor

Finally, UMI requires local weather data for conducting energy simulations properly. This data comprises fundamental climate properties specific to the location, including hourly temperature, humidity, solar radiation, wind direction, and speed. The precision and currency of weather data are vital for a thorough analysis of a UBEM within its natural environment. In recent years, the developers of UMI have introduced an online platform known as UBEM.io (Ang et al., 2022). This platform streamlines the process of UBEM creation through a user-friendly website. Users can insert building footprints and templates to generate a UBEM for analysis. UBEM.io offers functionalities for assessing the simulated UBEM, particularly in the context of retrofitting and carbon reduction strategies.

2.2 Data-Driven Models

2.2.1 Multiple Linear Regression

Multiple linear regression is a data-driven method used to model the linear relationship between a dependent variable and two or more independent variables [23]. In this approach, the dependent variable r is considered a continuous value, assumed to be generated by a deterministic function $f(x)$. This function calculates the sum of the linear combination of independent variables (inputs) and random noise ε (Equation 1) [23]:

$$r = f(x) + \varepsilon \tag{1}$$

If the noise occurs in a random process, it can be modeled as a Gaussian distribution with zero mean and constant standard deviation. Considering the output function is likely to have the same distribution as the noise, the dependent variable can be modeled as another Gaussian distribution, where the mean is an estimation based on the given input that has an index from 1 to m. To determine the output function $f(x)$, an estimator $g(x)$ is constructed with unknown parameters θ_i and θ_0 when the random noise is assumed to be zero (Equation 2):

$$g(x|\theta) = \theta_0 + \sum_{i=1}^{m} \theta_i x_i \tag{2}$$

The aim here is to find the parameters of the estimator. These parameters are derived using the maximum likelihood estimation by minimizing the error between the dependent variable r and the estimation y. The error function in Equation 3 is known as Mean Squared Error, where N represents the total number of observations, and X is the overall input matrix:

$$E(\theta|X) = \frac{1}{2} \sum_{t=1}^{N} (r^t - y^t)^2 \tag{3}$$

Another standard error metric in regression is MAPE, which measures the accuracy of a regression model by calculating the average percentage difference between the predicted and target values (Equation 4). MAPE represents the average percentage error across all predictions. A lower MAPE indicates better accuracy. For example, a 0% MAPE indicates a perfect fit between the predictions and targets. However, MAPE is sensitive to zero values in the target since it involves division by target values.

$$MAPE = \frac{1}{N} \sum_{t=1}^{N} \left| \frac{r^t - y^t}{r^t} \right| \tag{4}$$

2.2.2 Long Short-Term Memory (LSTM) Networks

Artificial Neural Networks (ANN) operate on the Multi-Layer Perceptron (MLP) algorithm, where features are assessed as individual sets (input layers), not collectively as a dataset. This allows MLP to iteratively update model weights based on the loss calculated for each input layer, an approach known as Online Learning [23]. To illustrate, consider a binary classification problem, where a possible outcome is zero or one, with a simple MLP model involving one hidden layer (Figure 4). During the forward-pass calculation, the model predicts the possible outcomes y_1 and y_2 using Equation 5:

$$y_i = f(w_{0i} + \sum_{j=1}^{n} x_j w_{ji}) \tag{5}$$

Here, m represents the number of features, w_{0i} and w_{ji} are the model weights, and $f(w, x)$ is the activation function. In each iteration, the model computes the weighted sum of features, applies an activation function (usually nonlinear) to transform them, and subsequently makes predictions. The MLP then calculates the error between the prediction and the target value. The model determines a gradient from this error and updates the weights using backpropagation. This cycle is repeated until the error falls within an acceptable range.

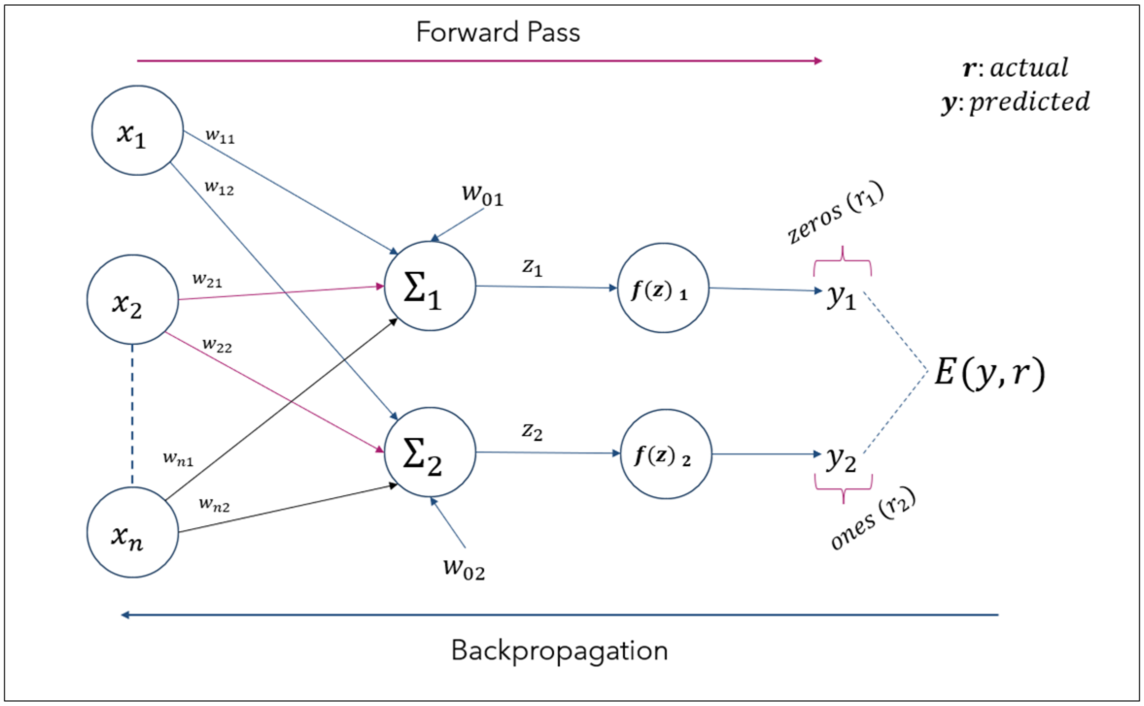

Figure 4 : A simple MLP architecture for classification

Classical feed-forward models, such as ANNs, cannot capture time-dependency in data. Consequently, when the target variable exhibits variations highly dependent on time, the limitations of these models become apparent. Hence, a necessity for sequence modeling arises. Recurrent Neural Networks (RNNs) are designed for sequential data. They include a hidden state to capture information from previous time steps [24]. However, classical RNN models face challenges in managing long-term dependencies and retaining sequential memory [25]. The capability to capture long-term dependencies is crucial in time-series analysis, but RNNs encounter difficulties as the influence from distant time steps decreases during training, mainly due to the vanishing gradient problem. Gradients become extremely small during back-propagation as the sequence length increases. Hence, the vanishing gradient complicates the model's learning process and makes capturing and utilizing information from earlier time steps challenging [26].

Long Short-Term Memory (LSTM) network represents an advanced RNN type designed to overcome these challenges [27]. LSTM models incorporate memory cells equipped with gating mechanisms, including input, forget, and output gates. These gates enable the model to store, discard, and output temporal patterns at each time step (Figure 5). This architecture mitigates the vanishing gradient problem and allows LSTM models to learn and maintain patterns across extended sequences. Consequently, LSTMs are widely used in time-series analysis tasks, such as stock price prediction [2], weather forecasting [28], and building energy consumption estimation [29].

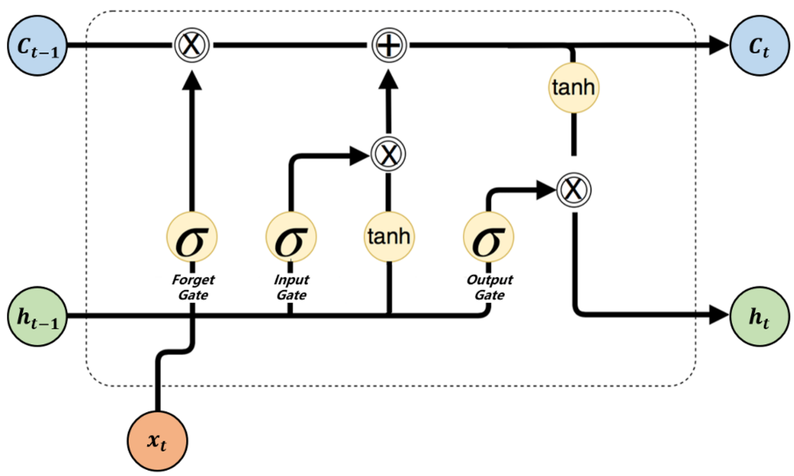

Figure 5 : The structure of the LSTM neuron. Retrieved from [2]

2.2.3 Bayesian Optimization

Bayes' formula, named after Thomas Bayes, is a mathematical formula that describes the probability of an event based on its prior knowledge conditioned by some external factors [30]. The decision theory adopted by this formula assumes updating and refining the posterior probability of the event by incorporating new evidence [23]. Bayesian Optimization begins with the fundamental concept of conditional probability. Conditional probability examines the probability of an event occurring, given that another event has already occurred. Mathematically, this is represented as $P(A|B)$, denoting the probability of event A occurring given the occurrence of event B [31]. This conditional probability can be expressed by Equation 6:

$$P(A|B) = \frac{P(A \cap B)}{P(B)} \tag{6}$$

Here, $P(A \cap B)$ is the probability is the probability that events A and B occurred simultaneously. This intersection set covers the conditional probability of event A occurring while event B has already occurred and vice versa [23]. Thus, we can write the following equations using Equation 7:

$$P(A \cap B) = P(A|B)P(B) = P(B|A)P(A) \tag{7}$$

From Equation 7, we obtain the Bayes' Formula, which plays a pivotal role in Bayesian reasoning. It is an expression derived from conditional probability and helps us update our beliefs as new information becomes available. The Bayes' Formula is given in Equation 8 [31]:

$$P(A|B) = \frac{P(B|A)P(A)}{P(B)} \tag{8}$$

Here, $P(A|B)$ is the posterior probability that we try to estimate, $P(B|A)$ is the likelihood, $P(A)$ is the prior probability of event A, and $P(B)$ is the evidence, representing the marginal probability of event B. Hence, Bayes' Formula can also be expressed as in Equation 9:

$$\text{Posterior} = \frac{\text{Likelihood} \times \text{Prior}}{\text{Evidence}} \tag{9}$$

Bayes' Formula allows us to estimate posterior probabilities based on prior knowledge and new evidence. It is a powerful tool for systematically updating our beliefs.

Based on Bayes' Formula, Bayesian Optimization is a probabilistic model-based optimization method for optimizing complex functions [30]. The primary objective of Bayesian Optimization is to minimize or maximize the error by determining the best parameter combination for a model [32]. Each parameter is considered a random variable with a specific probability distribution. Bayesian Optimization systematically explores the entire parameter space over the joint distribution of these random variables. It seeks optimal values for each parameter and attains a final parameter combination that optimally aligns with the objective function [30].

CHAPTER III

LITERATURE REVIEW

There are different approaches to analyzing how buildings use energy at the urban level. In the context of residential buildings, Swan and Ugursal classified these approaches into two types: top-down and bottom-up [10]. The top-down approach relies on historical data to make predictions. It examines the overall energy consumption of urban building stocks to create long-term plans considering urban planning and economic and technological growth strategies in cities. Because the goal is to understand general trends, the input data for top-down models can be broad, which include basic information for a district, like demographics (e.g., household income or employment rate), climate conditions, and general statistics from the construction industry (e.g., rental prices and construction costs) [10].

On the other hand, the bottom-up approach focuses on understanding the factors influencing the energy consumption of urban building stocks [10]. Its goal is to develop energy reduction strategies for building stocks at the urban or district levels. This method demands in-depth insights into regional climatic conditions and the characteristics of the buildings and occupants within the chosen district. Bottom-up urban building energy models can identify potential savings through various retrofitting strategies across building, occupant, and grid components, contributing to a reduced environmental impact in the built environment [11]. A solid bottom-up model facilitates scenario testing for urban energy efficiency benefits by understanding building energy characteristics and the factors influencing energy consumption.

Bottom-up models include statistical and dynamic models. Statistical models explore the impact of district demographics, climate characteristics, and building stock properties on energy consumption. These models use sophisticated data-driven techniques to distinguish factors influencing building energy use and predict future consumption [14]. Furthermore, they offer value by extracting meaningful insights, such as clustering buildings based on energy consumption behaviors or benchmarking buildings according to energy performance [33]. For example, Miller and Meggers employed machine learning techniques, such as classification for building performance and clustering for outlier detection, to transform the raw electrical meter data to create temporal features [34]. Similarly, Geraldi and Ghisi used clustering to determine the optimal number of archetypes representing the energy consumption characteristics of school buildings in Brazil [35].

3.1 Statistical Models

Statistical models aim to predict building energy use by correlating building properties, weather, and occupancy components with metered data. These models analyze building energy use at various spatial (neighborhood, district, or city level) and temporal resolutions (e.g., annually and monthly). Machine learning models are vital tools for statistical models to derive meanings from the input data, the combination of building characteristics and energy consumption, and perform predictions accordingly. However, these models usually cannot equip the time-dependent variables, such as building operational schedules and climate data. Thus, the energy consumption predictions of statistical models are usually at a low temporal resolution (e.g., monthly) while ignoring the hourly variations in the energy consumption patterns.

For example, Ma and Cheng used a Random Forest (RF) regressor to estimate the annual operational energy consumption of the buildings in New York [36]. They separated buildings into building groups according to the location and performed regression for each group. Building-specific properties and demographic characteristics of the household within a building group were the features of the models, for which they achieved a minimum of 0.78 MSE. Moghadam et al. developed linear regression models to estimate a building stock's daily space heating consumption in Italy [37]. Despite the promising regression results with a coefficient of determination (R-squared) value of 0.84, they generalized the building characterization due to the lack of available data. They also did not consider the climate conditions for daily predictions. Koschwitz et al. evaluated climate conditions and building operation schedules to predict the cooling and heating energy consumptions for two hundred buildings in Germany through Support Vector Machine (SVM) regression and Recurrent Neural Network (RNN) models [38]. Even though the predictions were in hourly resolution, they presented only the aggregated results for the different seasons of the year, where the RNN model outperformed the SVM regression with the least Mean Absolute Error (MAE) of 2.39. Touzani et al. performed a comparative analysis using different regression models to predict the monthly electricity consumption of over four hundred commercial buildings in the United States [39]. The Gradient Boosting (GB) regressor outperformed the other models with a 0.88 R-squared value. However, the 6-month training period for building the GB regressors provided slightly lower accuracy than the 12-month training period. Kristensen, Brun, et al. used a log-linear regression model to predict the annual heating energy consumption of single-family houses in Denmark [40]. The study covered over 10,000 buildings, which were utilized for the regression model's training, validation, and testing phases. Applying a basic archetype characterization yielded a 24% MAPE in the annual predictions.

In another statistical approach in UBEM, Abbasabadi et al. developed two models for assessing the annual energy use of over 58,205 urban buildings in Chicago [41]. The first model focused on building operational energy consumption. In contrast, the second model combined building energy use and transportation energy use per household, obtained from data like vehicle average miles per gallon and average passenger transportation energy intensity per mile. With the help of utilizing various machine learning models, the individual model achieved a minimum 1.81% MAPE with K-Nearest Neighbors (KNN) Regression, and the integrated model yielded a 4.10% MAPE with MLP Regressor. Gassar et al. analyzed the energy consumption of buildings within low and medium-populated areas in London using several regression models [42]. They highlighted the significance of socio-demographic, economic, and building properties as predictors for building operational energy, achieving an R-squared value of up to 0.99 with the MLP regressor. However, the predictions were in annual resolution and need to be updated since the building characterization and model validation were based on data obtained from the UK Census 2011. W. Wang et al. developed multiple regression models to predict electricity consumption across 56 buildings in various regions of a university campus in China [43]. The RNN model generally outperformed the MLP and SVM regressors and achieved an average of 6.66% MAPE in monthly building electricity use predictions. Nevertheless, the models needed more consideration for climate conditions and occupancy schedules, potentially impacting the monthly predictions' accuracy. W. Wang et al. predicted of operational building energy consumption at the building and urban levels in China [44]. The urban-level model employing the RNN algorithm performed better than other data-driven models and achieved an average MAPE of 6.5%. It should be noted that these predictions are in monthly resolution, and a limitation arises from the absence of occupancy-related information in the models.

The literature highlights the ongoing challenge of achieving accurate predictions with statistical models at higher spatial and temporal resolutions. The complexity arises from variations in building morphology, occupancy schedules, and weather conditions at the urban level. Additionally, the absence of building-specific input data and the limited availability of higher-resolution validation data (e.g., hourly metered consumption data) constrain statistical models. These complexities lead to analyses typically conducted at lower temporal resolutions for the statistical UBEMs.

3.2 Dynamic Models

Unlike the statistical model, dynamic models can capture the time-dependent variations in building operations, including the weather conditions and occupant behavior. There are mainly two dynamic models in building energy simulation: (1) physics-based and (2) reduced-order models. Physics-based models can provide accurate energy use prediction across higher spatial and temporal dimensions by analyzing buildings in multi-thermal zones and in elaborate time intervals. This accuracy renders them suitable for monitoring and controlling building energy use in urban contexts where spatial and temporal interactions are vital. However, these models are computationally intensive.

In contrast, reduced-order models offer an alternative by making a trade-off between the computational efficiency and the necessary precision in results. These models simplify the dynamic approach, reducing computational complexity while maintaining reasonable accuracy [45]. A study's scope and objectives should guide the choice between physics-based and reduced-order models. Table 1 outlines the most frequently used dynamic simulation tools in urban building energy modeling (UBEM) studies. For a more in-depth exploration of UBEM tools, readers are directed to the comprehensive study conducted by Ferrando et al. [7].

Table 1 : Most common UBEM tools

UBEM Tool	Developer	Model Type	Open Access
UMI [1]	MIT Sustainable Design Lab	Physics-Based	TRUE
TEASER [46]	RWTH Aachen University	Reduced-Order	TRUE
City Energy Analyst [47]	ETH Zurich	Reduced-Order	FALSE
CityBES [48]	Lawrence Berkeley National Laboratory	Physics-Based	TRUE

Modeling groups of buildings at either district level is challenging due to the infrequency of detailed input and validation data. As a result, dynamic models often employ the archetype approach, where archetypes represent clusters of buildings with similar characteristics, simplifying the creation of building energy models for the broader urban context. Archetype characterization comes in deterministic and probabilistic methods. The deterministic archetype characterization utilizes the plain version of the input data as the primary source. It identifies the details in the building's morphology and operational schedules by generalizing the input data. However, misrepresenting buildings within a cluster may lead to poor simulation results without comprehensive uncertainty analysis and up-to-date input data. Since metered consumption data and detailed building characteristics are rarely found, studies employing deterministic characterization cannot usually provide simulation results accurately and at high-temporal resolution.

For an example of deterministic characterization, Österbring et al. used a reduced-order model to analyze the heating consumption of 433 multi-family dwellings in Gothenburg [49]. The model simulated the annual heating consumption with a 3.0% MAPE. However, there are uncertainties on the reliability of the data used in building characterization and result validation. Buffat et al. simulated the annual heating consumption of 174 buildings in Switzerland with up to 0.6 R-squared value [50]. However, the simulation results needed to be more satisfactory since the results were at the annual resolution, and notably, there was no model calibration. Buckley et al. created a physics-based model to simulate the building's operational energy use and develop carbon reduction strategies for 9,000 residential buildings in Dublin [9]. The validation data was based on a domestic building energy assessment procedure, and the dynamic model simulated the annual energy use with a 15.6% MAPE overall. Even though the annual simulation results fell short of satisfactory, the proposed retrofitting strategies showed the potential to reduce future greenhouse gas emissions by up to 60%.

Some studies are dedicated to simulating hourly energy consumption through deterministic archetype characterization, but there are uncertainties in these studies' model calibration and validation. For example, Chen et al. developed a physics-based model to analyze the operational energy use of 940 buildings in San Francisco [51]. They focused on assessing the impact of retrofitting scenarios on energy reduction. However, despite simulating hourly energy consumption, they did not validate the model against the metered data. Likewise, Schiefelbein et al. used a reduced-order dynamic model to analyze the space heating consumption of buildings in Germany [52]. However, the results were not validated. Yang et al. created a physics-based model to investigate the heating consumption of over a thousand buildings in Leiden [53]. They gradually increased the model's complexity by incorporating weather data, refurbishment details, and occupant-related parameters into the archetypes. The final model simulated hourly heating energy consumption with a 31% Coefficient of Variation of the Root Mean Square Error (CVRMSE). However, there is room for improvement in the obtained results since the dynamic model was not calibrated.

On the other hand, probabilistic archetype characterization involves identifying parameters with the highest uncertainty and adjusting their values to achieve the desired simulation accuracy against metered data [54]. This method allows for representing building properties and operational schedules by capturing their variable nature rather than relying on fixed values. However, careful consideration is essential when defining potential values for archetype parameters. This requires domain expertise and reliance on building stock literature, such as building inspection surveys, building energy audit reports, and building energy standards [55] [56]. When applied appropriately, probabilistic archetype characterization yields reliable simulation results. Nonetheless, delivering high-temporal-resolution simulation results remains challenging for studies employing this approach because it is difficult to access hourly metered data and detailed building properties at the urban scale.

For instance, using a physics-based model, Cerezo et al. conducted a comparative analysis of deterministic and probabilistic archetype characterizations UBEM [57]. They focused on evaluating the annual operational energy use of residential buildings in Kuwait. The researchers calibrated the model using a form of Bayesian optimization designed explicitly for probabilistic archetype characterization. Through an annual calibration process that addressed occupant-related parameters, they achieved a notable reduction in the MAPE by up to 3% for the validation region, covering 159 buildings. However, the simulation results were at the annual resolution. Sokol et al. analyzed the monthly natural gas and electricity consumptions for 2663 residential buildings in Cambridge by employing a physics-based model [58]. The researchers implemented Bayesian optimization for model calibration at monthly and annual resolutions. When subjected to monthly calibration, the model demonstrated the lowest error with a 44% MAPE, which indicates the need for further improvement. Krayem et al. examined the operational energy consumption of various districts in Beirut through a physics-based model [59]. They identified occupant-related parameters as the primary contributors to the difference between simulation results and metered data. Consequently, they calibrated the model by manipulating the occupancy schedules at monthly and annual resolutions and reduced the simulation error by up to 3.4% in Root Mean Square Error (RMSE) at the monthly resolution for the district with 1830 buildings. Nevertheless, it is crucial to note that the model calibration needs to cover parameters other than building occupancy-related ones. C. Wang et al. developed a physics-based model to analyze the annual heating consumption of 84 residential buildings in Amsterdam [60]. They utilized Bayes optimization to calibrate the model and reduced the simulation error by up to 7.7% MAPE. However, the model performace was evaluated only at the annual resolution. Similarly, Gholami et al. developed a physics-based model to assess the annual operational energy use of 1156 buildings in Bologna [61]. The researchers utilized Bayesian optimization for model calibration and achieved a simulation error of approximately 2.53% MAPE at the annual resolution. Abolhassani et al. used a physics-based model to simulate the monthly cooling consumption of 35 buildings in Montreal [62]. The window-to-wall ratio (WWR) and internal heat gain of the archetypes were altered during the calibration, which caused the reduction of the simulation error to 15% of CVRMSE. However, archetype characterization and model calibration hold uncertainties.

The probabilistic archetype approach can expand the performance of dynamic UBEMs in analyzing the building energy consumption at the hourly resolution when the available validation and input data allow investigating the building energy consumption patterns at high temporal and spatial resolutions. For example, Kristensen et al. utilized a reduced-order model to examine the heating energy consumption of single-family houses in Denmark [63]. Using Bayesian optimization for model calibration, they simulated the hourly energy consumption for 18,475 buildings. The simulation results with the city-wide calibrated model demonstrated a MAPE of 11.8%. Likewise, Kristensen et al. introduced a multi-level calibration approach for a physics-based model that evaluates the heating energy consumption of residential buildings in Denmark [64]. They used Bayesian optimization to calibrate the model at the building and archetype levels. In the archetype-level calibration, the model simulated the three-hourly energy consumption of 100 buildings with a 7.8% CVRMSE. Hedegaard et al. formulated a physics-based model for evaluating the space heating consumption of 159 residential buildings in Denmark [65]. They utilized Bayesian optimization to calibrate the model by altering its archetype parameters and simulated hourly space heating consumptions with a 5.8% CVRMSE. Subsequently, the calibrated model was used to manage peak-hour demands in domestic hot water (DHW) consumption.

Even though obtaining reasonable simulation results is possible at the urban scale, dynamic models require a significant quantity of resources in terms of computation and time. Plus, these models are highly challenging to incorporate with the validation data and input data, such as building characteristics, operational schedules, and location-specific climate data, due to the need for more comprehensive information at the urban level. When the archetypes are not characterized properly, dynamic models lose the power to perform robust simulations considering thermal interaction between buildings and hourly fluctuations in building energy consumption patterns.

3.3 Hybrid Models

Researchers increasingly adopt hybrid approaches that blend statistical and dynamic models in UBEM due to efficiency and accuracy at high temporal and spatial resolutions. These models can either involve comparing the individual performance of statistical and dynamic models or integrating their functionalities into a unified method. The former aims to independently distinguish each model type's strengths and weaknesses, while the latter seeks to synergize their capabilities for a more comprehensive understanding of urban building energy dynamics.

In a comparative hybrid model, Nagpal and Reinhart compared statistical and dynamic models to evaluate the operational energy use of a campus building in Cambridge [66]. They used a simple linear model based on building areas and use types and a dynamic model to assess annual operational energy use intensities. When validated against metered data, the statistical model achieved an R-squared of 0.85, while the dynamic model performed even better with an R-squared of 0.96. Nageler et al. compared statistical and dynamic models by examining the daily heating energy use in a residential area with 34 buildings in Austria [67]. The non-linear regression model outperformed the dynamic model with an R-squared value of 0.97. Moghadam et al. compared statistical and dynamic models for analyzing the annual heating energy consumption of buildings in Turin [68]. The dynamic model outperformed the statistical model, exhibiting less than 10% MAPE when validated against metered data. Subsequently, the dynamic model was employed to evaluate energy reduction strategies across the city.

As an integrated hybrid approach, Nouvel et al. evaluated the annual heating energy consumption of more than 1000 buildings in Rotterdam [69]. They measured the precision of both dynamic and statistical models against metered data and with a 5-25% MAPE range. The dynamic model was subsequently employed to evaluate refurbishment scenarios to lower overall building energy consumption. Braulio-Gonzalo et al. examined how urban morphology affects the energy performance of buildings in Spain [70]. They identified three archetypes representing the characteristics of the region's building stock. Using a dynamic model, they simulated buildings with various parameter combinations and observed the distribution of target variables such as heating and cooling use and comfort hours. The simulation results were utilized to generate synthetic validation data. Subsequently, a statistical model was created using the integrated nested Laplace approximation (INLA) method. This model predicted target variables annually with a 0.63 Root Mean Square Error (RMSE) in cooling energy use prediction. However, the study needed metered data to validate the proposed models. Nutkiewicz et al. merged statistical and dynamic models to examine the energy consumption of 22 university buildings in California [71]. The dynamic model generated hourly electricity consumption data, which was used for validation. Then, the statistical model, incorporating a deep learning algorithm, namely Convolutional Neural Network (CNN), predicted electricity use at hourly, daily, and monthly intervals with MAPE values of 12.7%, 9.31%, and 8.28%, respectively. Nevertheless, the statistical model was not validated against metered data. Brøgger et al. developed a hybrid model to analyze the heating energy consumption of 134,065 residential buildings in Denmark [18]. The metered data from these buildings were split into training and test sets. During the training phase, the annual heating energy use simulated by the dynamic model served as validation data for the statistical model. The performance of both the dynamic and hybrid models was assessed using the test set, revealing MAPE values of 51.1% for the dynamic model and 31.2% for the hybrid model. It should be noted that the weather data was not included when developing the statistical model. Yi and Peng created a hybrid model to assess the energy performance of 659 residential buildings in Seoul [16]. They created multiple dynamic models representing different city districts and calibrated the archetype parameters affecting the building's internal loads and indoor air temperature. Combining these districts, the researchers then developed a statistical model at the urban level and predicted the monthly cooling energy consumption of the buildings with 0.969 R-squared. However, the parametric calibration needed to be elaborated, and the predictions were made in a single month in the study.

In another integrated hybrid study, Pasichnyi et al. developed different models to analyze the building energy performance and improve the electricity grid management in Stockholm [72]. They first calibrated a dynamic model for district-level retrofit assessments. Subsequently, using the archetypes from the dynamic model, they created a quasilinear regression model to predict hourly heating energy use for over six thousand buildings across the city, with an R-squared value of more than 0.75. However, the peak power estimation in the statistical model assumes that buildings using electric heating have similar load profiles as those connected to district heating. This assumption introduces uncertainty and requires a validation study using high-resolution metered data for individual buildings. Additionally, details about the dynamic model's calibration should have been provided. Roth et al. developed a hybrid model to evaluate the hourly energy demand of New York's building stock using data from 15,000 buildings [19]. The statistical model predicted annual electricity consumption with a 0.293 MSE, forming the foundation for a dynamic model. Utilizing optimization, they matched existing simulation results of reference buildings from a national study [73] to identify the most suitable load profiles. When validated against metered data, these load profiles yielded hourly electricity consumption with a

6.32% MAPE. While the statistical model is broadly applicable using publicly available data, the absence of an actual dynamic model for simulating buildings with their unique characteristics is noteworthy. Additionally, validation at an aggregated hourly resolution emphasizes the necessity for district or building-level validation due to urban variations, such as building density and morphology. In the most recent integrated hybrid study, Ali et al. analyzed the operational energy consumption of residential buildings in Ireland [17]. They employed a dynamic model to simulate the annual building energy consumption and generate synthetic validation data for the statistical model. They tested various data-driven algorithms to predict energy consumption by end-use, and the final statistical model achieved a 3.9% MAPE. However, a limitation is the absence of verification for synthetic validation data against metered consumption data. Table 2 summarizes the hybrid models in UBEM.

The observed literature shows that offering accurate energy consumption data at higher temporal resolution (e.g., hourly data) is still challenging for UBEM. Data generated from urban building energy simulations at lower temporal resolutions, like monthly or annual resolutions, is crucial for shaping the long-term planning of a city's building stocks and infrastructures. Urban planning authorities can use this data to analyze overall energy consumption and create large-scale strategies for reducing building energy use over time. This enables them to optimize resource allocation at the district or city level and focus on broad energy reduction strategies for building stocks rather than individual buildings. However, while valuable for long-term planning, the low temporal resolution data offers limited insight into daily variations in building energy demand, potentially missing intervention opportunities during peak hours.

In contrast, hourly building energy consumption data offers insights into daily energy demand patterns. It enables the strategic identification of peak demand periods for effective urban planning interventions. The temporal granularity at an hourly level is essential for developing load-shifting plans that optimize energy utilization during peak and off-peak hours as it contributes to designing energy-efficient systems and effectively controlling the grid during high-demand periods. Moreover, closely monitoring the hourly energy consumption of a building is an essential part of intelligent facility management that ensures the occupant's comfort by observing the sudden variations in the heating, cooling, and lighting demands [74].

Table 2 : Hybrid UBEMs

Ref.	Hybrid Approach	Validation	Calibration	Temporal Resolution	Minimum Error / Evaluation Metric
[66]	Comparison	TRUE	FALSE	Annual	0.96/R-squared
[67]	Comparison	TRUE	FALSE	Daily	0.97/R-squared
[68]	Comparison	TRUE	FALSE	Annual	<10%/MAPE
[69]	Comparison, Integrated Model	TRUE	FALSE	Annual	5-25%/MAPE
[70]	Integrated Model	FALSE	FALSE	Annual	0.63/RMSE
[71]	Integrated Model	FALSE	FALSE	Hourly, Daily, Monthly	8.28%/MAPE
[18]	Integrated Model	TRUE	FALSE	Annual	31.2%/MAPE
[16]	Integrated Model	TRUE	TRUE	Monthly	0.969/R-squared
[72]	Integrated Model	TRUE	TRUE	Hourly	>0.75/R-squared
[19]	Integrated Model	TRUE	TRUE	Hourly	6.32%/MAPE
[17]	Integrated Model	FALSE	FALSE	Annual	3.9/MAPE

Understanding and controlling urban building energy use at higher temporal and spatial resolutions necessitates combining statistical and dynamic models. Statistical models effectively capture general building energy consumption patterns but can enhance their utility by incorporating time-dependent and space-dependent variables, such as occupant-related parameters and microclimate effects. On the other hand, dynamic models offer in-depth insights into the time-dependent variations in the building energy consumption patterns but face challenges in comprehensive validation and input data representation for the urban climate and morphology. Integrating elements from both models is promising for hybrid models, yet existing hybrid models often lack result validation or model calibration. Thus, a novel hybrid approach in UBEM is essential to address these limitations.

CHAPTER IV

DYNAMIC MODEL

4.1 Creating a UBEM

Özyeğin University campus was selected for the study. The campus is located in Çekmeköy, İstanbul. There are fourteen conditioned and one unconditioned building on the campus. However, one of the conditioned buildings, the OZU-X building, is under the ground surface. It is complicated to conduct building energy performance analysis for the OZU-X buildings since dynamic simulation tools consider the effect of solar radiation and wind on the building surface. Thus, the OZU-X building was removed from the study. The remaining buildings' total gross floor area (GFA) is $243,564$ square meters.

Clustering buildings into archetypes with similar energy characteristics is very important when working at the urban level, as a massive number of buildings might aggravate collecting building-specific data and, thus, performing detailed energy simulations. The remaining 13 buildings on the campus have different use types. In this sense, these buildings were clustered into four archetypes: academic building, dormitory, social building, and sports center. Table 3 shows the buildings and corresponding archetypes, and GFAs.

UMI, developed by MIT Sustainable Design Lab [75], was selected to perform dynamic energy simulations. UMI requires three main types of input data. These are building templates, building geometries, and weather data. A building template is text-based data that includes the essential characteristics of the building, such as the building envelope properties, zone conditioning details, HVAC details, domestic hot water (DHW) details, and building operational schedules. Each title requires a detailed description of the system or building part. For example, envelope properties are the material and construction details of the opaque and glazing surfaces, such as external walls and windows Figure 6.

Table 3 : Buildings, corresponding archetypes, and GFAs

Building Name	Archetype	GFA (m^2)
AB1	Academic Building	22,935
AB2	Academic Building	21,974
AB3	Academic Building	24,880
AB4	Academic Building	27,153
SCOLA	Academic Building	17,884
OM	Social Building	20,036
SM	Sports Center	13,317
Y1	Dormitory	10,723
Y2	Dormitory	11,136
Y3	Dormitory	13,766
Y4/5	Dormitory	24,459
Y6	Dormitory	29,450
GH	Dormitory	5,851

In zone conditioning, various parameters affecting the heat transfer in zones are given, such as heating and cooling set points and the efficiency of the heating and cooling systems (Figure 7). Building operational schedules cover the daily, weekly, and annual schedules for various occupant-related parameters, such as occupant density, equipment power density (EPD), lighting power density (LPD), mechanical and natural ventilation schedules, and zone conditioning schedules. The hourly daily schedules are represented as a density value between zero and one.

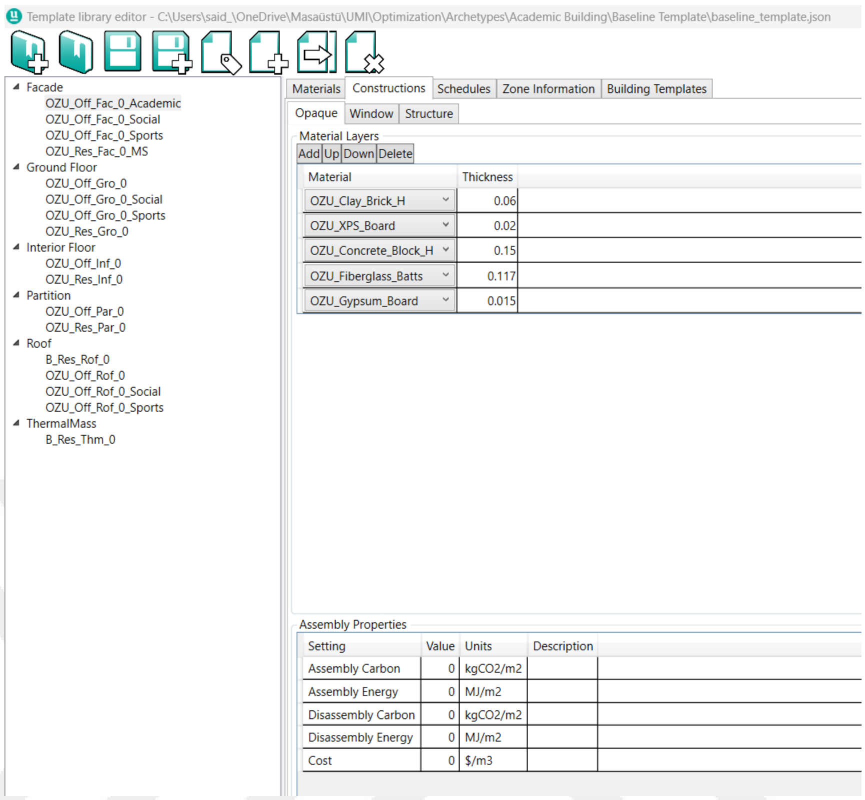

Figure 6 : Sample construction from UMI Template Editor

The input data required in a building template should represent the selected building to ensure the accuracy of the energy simulation. In this sense, necessary permissions to collect the available building data were obtained from the deanery. Two energy audit reports were conducted on campus in 2014 and 2020. These reports contain essential information about the energy performance of the buildings. In addition, the campus buildings' architectural, electrical, and mechanical plans were used to identify and characterize buildings in the study. Each piece of information was stored at the building level. However, some parameters required in UMI were not available in the energy audits, and determining them using the available data can be tricky. For example, deriving EPD and LPD for an entire building is a highly complex task since zones are used for different tasks (e.g., classes and cafeterias). Likewise, the infiltration rate, which denotes the air change in a zone per hour, is challenging to determine for an entire building, and it should be observed using sensors as the infiltration rate varies from the building shell to the core. Besides the parameters that involved uncertainty and were not present in the available data, all building recordings were processed, and archetypes were characterized using the UMI Template Editor.

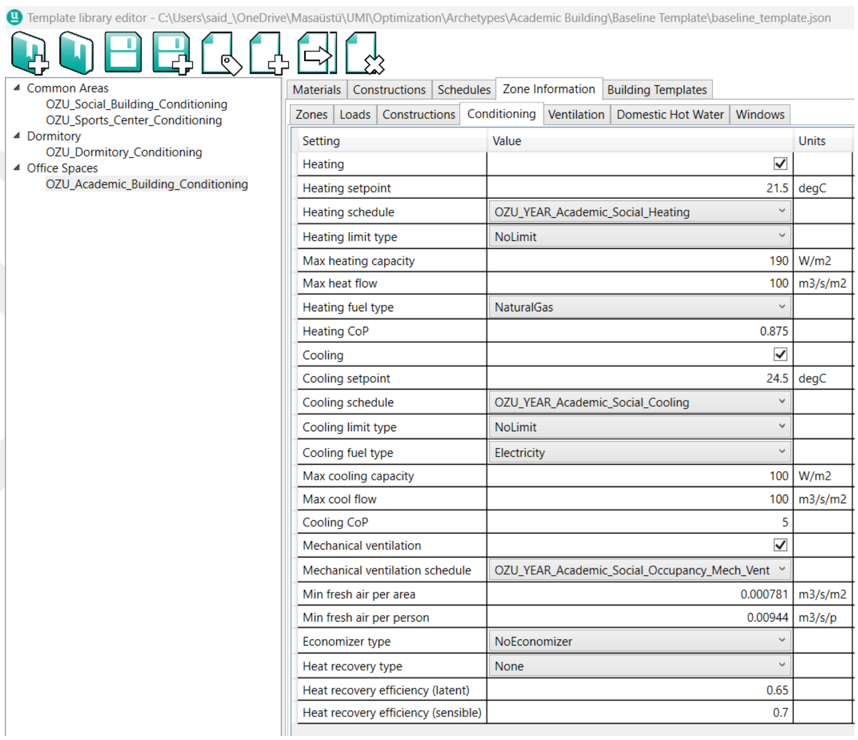

Figure 7 : Sample zone conditioning from UMI Template Editor

The next step was to create a 3D model of the campus. Yandex Map Constructor was employed to create building footprints. Yandex Map Constructor is a geographic information system application. It utilizes aerial images and transforms them into building footprints. Several polygons representing the footprints of the buildings on the map were drawn in Yandex Map Constructor. However, these footprints usually indicate the top floor plan. A building floor plan may vary significantly from floor to floor. Therefore, the evacuation plans for the separate floors of each building were utilized to check whether the footprints properly represent the buildings' geometry. Once each building footprint was extracted as a map layer, the final map file was extracted as a GEOJSON file. This file was then inserted into the UBEM.io tool, an online platform to create UBEMs [74]. UBEM.io consists of different work stages, such as forming building geometry from the footprint, assigning building templates to the building geometry, and creating a UMI file used in energy simulation. A GIS interface in UBEM.io ensured that the buildings were in valid coordinates and that the footprints were not overlapping. Then, building heights were inserted into UBEM.io, and a UMI file was obtained. Figure 8 shows the 3D model of the campus building in Rhino.

There is a significant elevation difference between the buildings on the campus. The Health, Safety, and Environment (HSE) department of Özyeğin Üniversity prepared evacuation plans for each building, in which they determined the quad area as the reference elevation (zero point). According to zero point, for example, the architectural faculty (AB4) has ten floors, and only three of them are above zero point. On the other hand, the engineering faculty (AB1) has eight floors, six of which are above zero point. However, due to the practical difficulties, the level of detail in 3D modeling should be kept simple or generalized at the urban level studies. Since this study aims to develop a generalizable approach to assess the energy performance of the urban building stocks, the elevation differences were not regarded. Instead, all buildings were assumed to rise from zero point with their exact height when creating a 3D campus model. However, the elevation differences between buildings can notably affect the wind flow and solar radiation. Hence, the thermal interaction between buildings can be altered. It is worth noting that an elaborate approach should be developed in creating building geometries for UBEMs.

The final input of the campus model is the weather data. There are multiple weather stations near campus. The deanery sent a formal request letter to the Turkish State Meteorological Service (TSMS) and asked for detailed weather data from the nearest station to the campus. The hourly weather data between September 2018 and

September 2023 was obtained from TSMS. These data include temperature, relative humidity, dew point temperature, wind direction and speed, sun exposure intensity, and total precipitation at the hourly resolution within the given years.

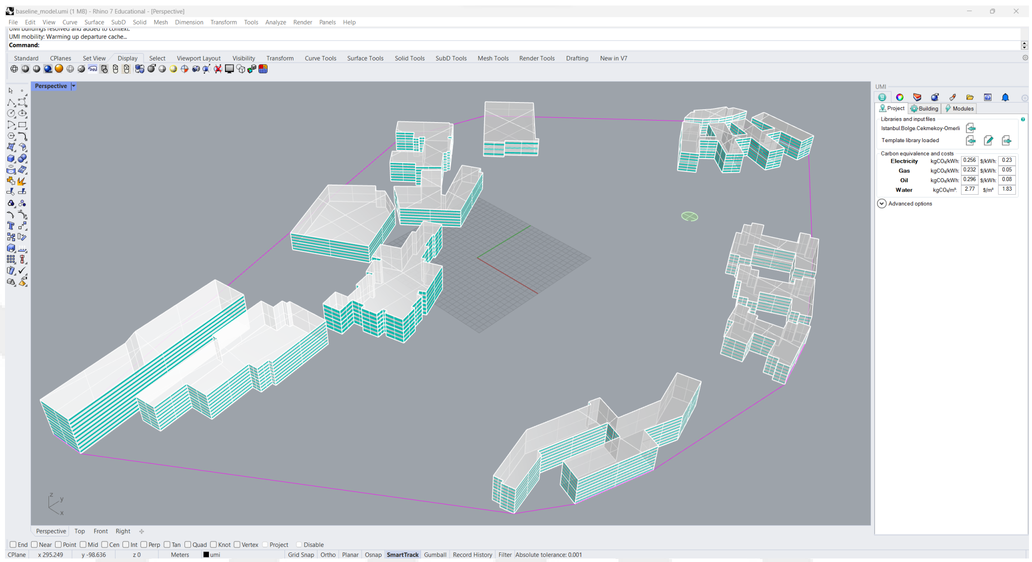

Figure 8 : 3D campus model in Rhino

4.2 Editing the validation data

The metered consumptions of the buildings form the validation data of the study. This data includes the natural gas and electricity consumption. The dynamic model created via UMI considers several end-uses when determining the energy consumption of the buildings. Among these end-uses, cooling, equipment, and lighting energy are provided with electricity, whereas heating and DHW are supplied by natural gas. The electricity consumption is recorded for each building with a specific electricity meter at the monthly resolution. Thus, there is detailed monthly validation data for electricity consumption. However, the university utilizes a district heating and cooling system with multiple stations throughout the campus, complicating obtaining the exact natural gas consumption per building. For example, central campus buildings, which are the academic building, social building, and sports center, are conditioned and supplied with hot water using the energy distribution center (EDC). Also, three dormitory stations supply heating and hot water to dormitories. Even if small air conditioners cool the offices of the authorized dormitory personnel, it is assumed that the dormitory buildings do not require cooling.

The natural gas consumption can be derived using the buildings' total GFA. Since the building's entire space is usually conditioned by the district system within operation hours, regardless of occupant density, the floor areas can be a good indicator of natural gas consumption. This assumption works for the dormitory buildings. The electricity grid and natural gas pipelines mainly supply the energy demand of the central campus buildings. Nevertheless, there is a trigeneration system at the EDC. The trigeneration system first burns the natural gas to produce electricity through a generator. The waste heat produced during electricity generation is then captured and utilized for heating or cooling. Simultaneously producing electricity, hot water, and chilled air reduces the overall energy consumption. The existence of the trigeneration system indicates that the metered data only partially reflects the building energy consumption. Therefore, the buildings' actual cooling, heating, and DHW consumption should be determined using the trigeneration effect since the waste heat energy supplies extra energy.

The details of the trigeneration system are available in the 2020 energy audit report. This system was established in early 2017 and has been actively used since the beginning of 2018. The system efficiency is 82.7%, according to the 2020 energy audit report. This suggests that the system's electrical power is around $1290kW$, as the maximum power is $1560kW$. There is a detailed table about the electrical and thermal efficiency of the system per electrical power. For example, in energy generation with a total capacity of 1569 kW, the trigeneration system generates electricity and waste heat with 42.3% and 41.0% efficiencies, respectively. From this table, the efficiency of the trigeneration system in generating waste heat was calculated as 41.98%. The generated electricity from the waste heat was stored and available per month.

Therefore, extra calculations were only made for the waste heat generation.

According to decision number 8301, published in the Official Gazette of the Republic of Turkey and aimed at determining the transmission and shipment control fees for Petroleum Pipeline Corporation (BOTAS) in 2019, $10.64kWh$ of energy is released from burning one cubic meter of natural gas. Hence, the trigeneration system generates $4.47kWh$ of waste heat energy by burning a cubic meter of natural gas. However, another complication occurs for the central campus buildings at this stage. There is some extra natural gas consumption on the central campus. For instance, the pool in the sports center needs to be heated throughout the day. Also, the kitchen in the dining hall requires a massive energy DHW consumption compared to the typical areas on the campus. Similarly, the practice kitchen and the restaurant at the applied sciences faculty consume a severe amount of DHW energy. It is not easy to represent these extra consumptions in the dynamic model. This is because the dynamic model divides buildings into a few zones and assumes that these zones have similar consumption patterns. Extra hot water consumption from pool heating, cooking, and washing dishes differs from the mentioned consumption patterns. Therefore, these extra natural gas consumptions should be determined carefully and removed from the final metered natural gas data.

The extra consumption is due to two main activities: pool heating and the DHW demand for the kitchens. The details about pool heating were obtained from the sports center officials. Energy Star released a technical report on analyzing the energy demand of swimming pools in the United States and Canada [76]. In that report, the pool energy consumption was expressed usingEquation 10:

$$E_{\text{pool}} = E_{\text{evaporation}} + E_{\text{convection}} + E_{\text{pump}} - E_{\text{solar radiation}} \tag{10}$$

The term E stands for energy in Equation 10. The solar radiation was assumed to be zero since the pool is an indoor pool located in the sports center. The parameters in Equation 10 were determined using the properties of the sports center and swimming pool, including the volume of the pool, air temperature set point, pool temperature set point, and the pool's operating hours. For example, the pool is constantly heated. Hence, the operating hours were assumed to be 8,760 in a year. The pool heating energy was calculated as $734,893 kWh/year$ using the formulations in the Energy Star report. This value was divided into twelve months equally to represent the monthly energy required to heat the swimming pool. Since the indoor air is conditioned in the sports center until late hours, the outside temperature variations were ignored when calculating the pool heating energy. The kitchen DHW use caused the subsequent extra energy consumption. UMI calculates the DHW energy in kWh using Equation 11:

$$Energy_{\text{DHW}} = \text{Flow Rate} \times \text{COP} \times \Delta_T \times \text{GFA} \times \text{DHW Schedule} \quad (11)$$

In Equation 11, COP represent the boiler's coefficient of performance, Δ_T stands for the temperature difference between the inlet and outlet water, GFA is the gross floor area in m^2, and $DHWSchedule$ is the annual operating hours of DHW. Here, the flow rate is the most significant parameter when calculating the DHW energy. The DHW flow rate is the maximum flow rate of the DHW systems, which is usually represented in $m^3/hours/m^2$ or $m^3/person/day$. Determining a precise flow rate is a complex task since there is a significant variation in the DHW operating schedules at different times of the day and at different times of the year. Therefore, a literature survey on the DHW consumption of restaurant buildings was conducted to derive reasonable DHW flow rates.

For example, Murakawa et al. analyzed the DHW demand for restaurant buildings in Japan and created sample flow rates per season and restaurant type [77]. In a national study, the U.S. Department of Energy (DOE) created typical building templates per state representing the local building and climate characteristics [73]. In DOE's study, a typical restaurant was simulated using the HVAC properties and operating schedules, which were gathered after elaborate research on the local building stocks. Pérez-Lombard et al. examined the DHW consumption of different building types and the effect of the DHW energy on the overall building operational energy in Europe and the USA [78]. Fuentes et al. (2018) created DHW flow rates for different building types using the operational schedules in Europe, Canada, and the USA [79]. The DHW flow rates per building type obtained from the studies mentioned above are given in Table 4.

Table 4 : DHW flow rates per building

Building Use Type	Minimum DHW Flow Rate (L/person/day)	Average DHW Flow Rate (L/person/day)	Maximum DHW Flow Rate (L/person/day)
Residential	29.50	54.12	94.00
Hotel	27.13	112.94	354.45
Office	2.77	3.87	4.45
School	1.89	4.39	7.19
Restaurant	3.20	12.44	21.00

It should be noted that the flow rates in Table 4 will be used as baseline values in the study's later stages when determining the archetypes' DHW consumptions. Extra consumption due to the DHW's use of the kitchens was calculated as the average flow rate of the restaurant. This information was combined with operational schedules of the dining hall, the practice kitchen, and the restaurant at the applied sciences faculty. Later, extra DHW consumptions were gathered with pool heating energy use to calculate the final extra energy consumption. Table 5 summarizes the extra natural gas consumption at the monthly resolution due to the pool heating and DHW use of several kitchens.

Table 5 : Extra Natural Gas Consumptions

Month	Swimming Pool (kWh)	Dining Hall DHW (kWh)	LCB - Practice Kitchen (kWh)	LCB - Restaurant (kWh)	Total Extra Consumption (kWh)
1	61,241	17,201	192	230	78,864
2	61,241	14,907	192	0	76,340
3	61,241	14,460	1,258	691	77,650
4	61,241	15,040	1,258	691	78,230
5	61,241	16,497	1,258	691	79,687
6	61,241	16,072	1,258	691	79,262
7	61,241	16,556	1,258	0	79,055
8	61,241	16,460	211	0	77,912
9	61,241	16,125	192	0	77,558
10	61,241	17,072	1,258	230	79,801
11	61,241	19,769	1,258	230	82,499
12	61,241	17,439	1,258	230	80,169

The trigeneration effect can now be assessed after determining the extra natural gas consumption from the pool heating and kitchens' DHW, which will not be simulated in UMI. Özyeğin University stores the energy consumption data separately as the natural gas used in direct zone conditioning and the natural gas used in electricity generation through the trigeneration system. Zone heating and DHW use are mainly sourced from the waste heat energy revealed during electricity generation. The natural gas from the pipeline is activated when the trigeneration system's waste energy is insufficient. It is very challenging to understand the precise natural gas consumption of the central campus buildings without knowing how much of the generated waste energy is utilized to heat the zones and domestic water in the buildings. Summer terms can be a good starting point in solving this challenge.

Algorithm 1: Trigeneration Calculations

```
if SEASON == SUMMER then
    if Summer DHW ≥ Utilized Waste then
        Waste Heating = Utilized Waste;
        Waste Cooling = 0;
        Heating Consumption = Pipeline + Waste Heating;
    else
        Waste Heating = Summer DHW;
        Waste Cooling = (Utilized Waste - Summer DHW) * Absorption Chiller COP;
        Heating Consumption = Pipeline + Waste Heating;
    end
end
else if SEASON == WINTER then
    Waste Heating = Utilized Waste;
    Waste Cooling = 0;
    Heating Consumption = Pipeline + Waste Heating;
end
else if SEASON == MAY then
    if Summer DHW ≥ Utilized Waste then
        Waste Heating = Utilized Waste * 0.5;
        Waste Cooling = 0;
        Heating Consumption = Pipeline + Waste Heating;
    else
        Waste Heating = Summer DHW;
        Waste Cooling = (Utilized Waste - Summer DHW) * Absorption Chiller COP *
          0.5;
        Heating Consumption = Pipeline + Waste Heating;
    end
end
```

Figure 9 : Pseudo code for the trigeneration calculations

During the summer term, there is no zone heating. The only natural gas demand is caused by DHW use during summer. So, if a minimum DHW consumption can be determined for the buildings, the waste energy from the trigeneration system can be divided into Waste Heating and Waste Cooling for the summer season. Using the DHW flow rates of the academic building from Table 4, the operation schedules for the academic buildings, and the GFA of the buildings, a baseline DHW energy consumption for the central campus was calculated for the summer season. According to this, the central campus buildings were assumed to consume a minimum of $348,321 kWh$ of energy during summer. This assumption also works for the entire year. However, for example, all the waste energy generated by the trigeneration system is utilized to heat the zones and domestic water in winter. Therefore, waste heat energy is assumed to inherently include the minimum DHW consumption. The winter season is between October 1 to May 15. The summer season is between May 16 and September 30. Due to the temperature drops in the last few years, May was assumed to have undergone both heating and cooling. The trigeneration effect was calculated according to the Summer, Winter, and May seasons. The summary of the trigeneration calculations is given in Figure 9. The naming in the trigeneration calculations requires explanation. For example, the utilized waste energy was calculated in Equation 12:

$$\text{Utilized Waste} = \text{Generated Waste} - \text{Extra Consumption} \tag{12}$$

In Equation 12, the generated waste represents the total waste heat generated by the trigeneration systems, whereas the extra consumption indicates the extra energy used from pool heating and kitchens' DHW use. The trigeneration system generates $4.47 kWh$ of waste heat energy by burning a cubic meter of natural gas. The total generated waste heat energy was calculated monthly using the natural gas consumption used for the trigeneration system. Then, the utilized waste energy was calculated by subtracting the extra consumption from the generated waste energy (Equation 12). Summer DHW indicates the minimum DHW energy use required in the summer season. Waste heating and waste cooling are energy uses supplied from the utilized waste energy of the trigeneration system. Absorption Chiller COP represents the efficiency of the absorption chiller device that uses the waste energy for cooling purposes. Finally, heating consumption is the total heating use of the buildings determined by summing up the natural gas supplied from the pipeline and the waste heating energy. Likewise, the waste cooling energy calculated for each month was then added to the electricity consumption since the cooling demand on the campus was assumed to be supplied by electricity. The heating and cooling seasons of the campus, as well as conditioning schedules, were obtained from the university administration.

For the summer term, if the Summer DHW is less than the Utilized Waste, this means that the Utilized Waste can only supply the minimum DHW demand of the central campus. Therefore, all the Utilized Waste is used for Summer DHW, leaving zero energy for the Waste Cooling. However, when the Utilized Waste exceeds the Summer DHW, the trigeneration's waste energy is shared between the Summer DHW and Waste Cooling.

In May, trigeneration calculations are complicated since there are both cooling and heating for this month. Thus, half of the month was considered for heating, and the other half was for cooling. After this distinction, the regeneration calculations resemble the ones in the summer term. If the Summer DHW is greater than the Utilized Waste, all the Utilized Waste goes for the Waste Heating, but 50% of it since the heating takes only 15 days during this month. If the Summer DHW is less than the Utilized Waste, then the Utilized Waste is shared between the Waste Heating and Waste Cooling.

The trigeneration calculations get very simple when it comes to the winter term. This is because there is no cooling during winter. Thus, all the Utilized Waste is owned by the Waste Heating. The calculations in Figure 9 were performed for all the months between January 2018 and November 2023, and the final natural gas and electricity consumption data were derived for the central campus buildings.

However, it was only possible to use some of these consumptions as validation data due to some complications. For example, the hourly weather data obtained from TSMS covers only September 2018 and September 2023. Since the simulations will take this weather data as input, the simulation results will reflect the energy consumption based on this weather data. Moreover, the building energy consumption patterns on campus drastically changed during the pandemic since the buildings remained unoccupied for most of the pandemic. In addition, the trigeneration system was subjected to a resource optimization experiment between May and December 2022. During this period, the trigeneration system was either not used or operated at low capacity. Thus, the trigeneration calculations for this period contain significant uncertainty.

Month/ Year	1	2	3	4	5	6	7	8	9	10	11	12
2018	No Weather	No Weather	No Weather	No Weather	No Weather	No Weather	No Weather	No Weather	Included	Included	Included	Included
2019	Included	Included	Included	Included	Included	Included	Included	Included	Included	Included	Included	Included
2020	Included	Included	Pandemic	Pandemic	Pandemic	Pandemic	Pandemic	Pandemic	Pandemic	Pandemic	Pandemic	Pandemic
2021	Pandemic	Pandemic	Pandemic	Pandemic	Pandemic	Pandemic	Pandemic	Pandemic	Pandemic	Pandemic	Included	Included
2022	Included	Included	Included	Included	Trigen. Off	Trigen. Off	Trigen. Off	Trigen. Off	Trigen. Off	Trigen. Off	Trigen. Off	Trigen. Off
2023	Included	Included	Included	Included	Included	Included	Included	Included	Included	No Weather	No Weather	No Weather

Figure 10 : Choosing Validation data from the months of 2018 and 2023

Considering all of these, the remaining months that can be assessed in determining validation data are illustrated in Figure 10. In this table, the periods were classified as No Weather Data, Pandemic, Trigeneration Off, and Included. No Weather Data indicates the months with no hourly weather data. Pandemic shows the pandemic period, whereas Trigeneration Off represents the period when the trigeneration system was considered out of operation. Finally, Included represents the months that are utilized in validation data. The average natural gas and electricity consumptions between the included months constituted the validation data. Then, using the GFA of the central campus buildings, individual natural gas consumption per building was obtained.

4.3 Selecting important features for energy simulation

UMI simulation requires various information to characterize buildings and analyze their energy performance. This information includes the zone constructions (e.g., façade properties), ventilation settings (e.g., infiltration rate), zone conditioning settings (e.g., heating set point), zone loads (e.g., occupancy density), and DHW settings (e.g., DHW flow rate). Each category in a UMI building template involves important parameters and operating schedules that can affect building energy consumption. For example, the heating set point and the heating schedule parameters in the zone conditioning category determine to what extent and how often a zone will be heated. Likewise, in the zone loads category, the occupancy density and the occupancy schedule examine how often and with what intensity people use a building and calculate the internal heat gains resulting from these uses.

The operating schedules for heating, cooling, mechanical ventilation, natural ventilation, and DHW were obtained from the Özyeğin University. Ready-to-use UMI templates that could not be obtained from the university were utilized for the remaining operating schedules. Operating schedules are critical parameters of energy simulations in UMI, and deriving them is challenging because various factors cause uncertainty in building operations. For example, the lighting or equipment availability schedules may vary at different hours of the day and different periods of the year. Likewise, they might depend highly on the zone characteristics and occupant use. Thus, deriving these schedules needs elaborate research that involves monitoring a building's different zones with sensors.

Many urban planning studies employed UMI [74]. Since the UMI was developed for the urban context, these studies observed urban building stocks with different building types. Therefore, ready-to-use building templates in UMI include the characteristics of a wide range of building types. For example, the dormitory operating schedules (e.g., heating schedules) were inspired by the residential building templates available in UMI, in which heating is intense in the morning and night hours, whereas it is less intense in the afternoon and evening. Similarly, the operating schedules of the academic buildings were developed according to an office building in the UMI template, in which the zone conditioning is off outside of working hours.

The next step was to specify the deterministic parameters for the archetypes, such as the external walls' thermal transmittance rate (U-Value), heating set points, DHW flow rates, EPD, or window-to-wall ratios. Some of these parameters were obtained from the energy audit reports. However, specifying a particular value for each parameter was impossible. For example, equipment and lighting power densities may vary in the different zones of a building. Likewise, the infiltration rate, which refers to the amount of outside air that naturally enters the building from the cracks or openings, is challenging to be determined. This is because the outside air influences a building's shell and core zones differently. Therefore, the parameters that contain uncertainty should be examined in detail. However, considering the vast number of uncertain parameters, a feature importance analysis should be performed to select which parameters influence the building's energy consumption most. This brings us to the Sensitivity Analysis.

Besides the parameters with unknown distribution, some parameters can be detected using the available data sources. For example, the building envelope properties, such as U-Values of the external walls, roofs, and ground surfaces, were determined using the energy audit report. However, when creating archetypes, the average values of these parameters were considered. Even though the exact values for those parameters were obtained, it was impossible to represent every building with its specific characteristics in UBEM. Generalizing the building stocks and grouping them into archetypes is the essential point of UBEM due to the data acquisition problems and computational constraints in simulations. However, some information can be lost during this generalization. Therefore, the importance of the parameters should be adequately understood. Table 6 summarizes the parameters selected for the uncertainty analysis. In Table 6, the available parameter values of 13 buildings were analyzed. Here, the coefficient of variation (CV) for each parameter was utilized in the uncertainty analysis. The CV value is obtained using Equation 13:

$$CV = \frac{\text{Standard Deviation}}{\text{Mean}} \tag{13}$$

The CV value in Equation 13 determines how much the observations deviate from the sample average for a parameter. High CV values indicate a high uncertainty, whereas low values refer to low uncertainty. Table 6 reveals that the parameters in the zone construction category usually include low uncertainty. For example, the U-values of the external walls and windows have a relatively low CV value. The CV value of the Roof U-Value looks critical. However, there is a tiny difference between changing the Roof Value to its maximum and minimum in the practice. For example, the minimum and maximum U-Value for the roof construction are 0.30 and 0.56, respectively, corresponding to lower than five centimeters of insulation. In practice, five-centimeter insulation thickness alteration is neither quite possible nor necessary. On the other hand, the minimum and maximum U-Values of the ground constructions can change the energy consumption since there is more than a ten-centimeter difference in the insulation thicknesses. Therefore, only the Ground U-Value was assumed to have high uncertainty among the parameters in the zone construction category and selected for the sensitivity analysis.

The parameters in the zone conditioning category exhibit a very low CV. However, the CV value cannot be the only determinant of the uncertainty level of the parameters. In building energy simulation, conditioning the zone with heating and cooling comprises a significant part of the building energy consumption. The temperature set points of the zones and the efficiency of the heating and cooling systems require detailed attention. Thus, these parameters were selected intuitively for sensitivity analysis, even though the uncertainty analysis showed the opposite.

Table 6 : Uncertainty analysis for the simulation parameters

Parameter	Unit	UMI Template Category	Minimum Value	Maximum Value	CV
External Wall U-Value	$W/m^2/K$	Zone Constructions	0.27	0.39	0.16
Roof U-Value	$W/m^2/K$	Zone Constructions	0.30	0.56	0.30
Ground U-Value	$W/m^2/K$	Zone Constructions	0.30	1.74	0.59
Window U-Value	$W/m^2/K$	Zone Constructions	1.5	2.4	0.00
Scheduled Ventilation ACH	ACH	Ventilation Settings	0.1	1.0	Unknown
Infiltration	ACH	Ventilation Settings	0.1	0.5	Unknown
Heating Set Point	Degree Celsius	Zone Conditionings	20	23	0.10
Cooling Set Point	Degree Celsius	Zone Conditionings	23	26	0.08
Heating COP	%	Zone Conditionings	80	95	0.12
Cooling COP	-	Zone Conditionings	4.5	5.5	0.14
EPD	W/m^2	Zone Loads	5	15	Unknown
LPD	W/m^2	Zone Loads	5	15	Unknown
Occupant Density	$people/m^2$	Zone Loads	0.013	0.103	0.60
DHW Peak Flow Rate	$m^3/h/m^2$	DHW Settings	1.58E-05	7.09E-04	Unknown

The occupancy density, which is the number of people per square meter, in the zone loads category has a high CV value. Plus, this parameter can directly affect the internal heat gain of a zone since the activities of the building occupants can generate heat through metabolic functions, electronic device use, and lighting use

[80]. Therefore, the occupancy density was selected for the sensitivity analysis. Some parameters offer no prior knowledge about their distributions, such as the scheduled ventilation air changes per hour (ACH), infiltration rate, EPD, LPD, and DHW flow rate. These parameters inherently hold uncertainties since there is a significant variation in their distributions by time, occupancy density, and occupant behaviors. Thus, they were included in the sensitivity analysis. However, the possible values that these parameters can take should be determined. Scheduled Ventilation ACH represents the density of the natural ventilation initiated by the occupants. For example, when an occupant opens a window or a door in a building, the Scheduled Ventilation ACH changes. Thus, the possible densities for this parameter can be either one or zero, as the extreme points for a window condition are either open or closed.

The infiltration rate denotes the air change rate per hour. An infiltration rate of 1.0 means that the outside air replaces all the inside air in an hour. Since the buildings on the campus were constructed after 2010, they were considered new constructions. Thus, they were expected to have low infiltration rates due to the improved envelope insulation. However, a building's shell and core interact with the outside air at different levels and might have very different infiltration rates. Therefore, a safe and reliable value range of 0.1 and 0.5 was determined for the infiltration rate, suggesting that only half of the inside air can be replaced by the outside air per hour at most.

Another uncertainty exists for the EPD and LPD. Sensor monitoring per zone and inventory counting on all the electrical devices in a building should be performed to calculate precise power densities for EPD and LPD. Since it was not practical nor within the scope of this study, ASHRAE Templates from the DOE's study and ready-to-use UMI templates were investigated. Campus buildings have different use types, such as offices, residential areas, restaurants, and sports centers. Value ranges for LPD and EPD were created based on this diversity. Finally, findings from the literature review summarized in Table 4 were used to create possible DHW flow rates per archetype. These values are given in Table 7.

Table 7 : Possible DHW flow rates per archetype

Archetype	DHW Flow Rate (m3/h/m2) - Minimum	DHW Flow Rate (m3/h/m2) - Average	DHW Flow Rate (m3/h/m2) - Maximum
Academic Building	2.93E-05	7.02E-05	1.11E-04
Dormitory	1.56E-04	5.57E-04	9.58E-04
Social Building	2.65E-05	6.37E-05	1.01E-04
Sports Center	5.27E-05	1.10E-04	1.68E-04

In the sensitivity analysis, all the buildings on the campus were identified as academic buildings in the dynamic model to reduce the number of energy simulations due to computational and time constraints. This also facilitated observing the influence of a parameter in more detail, as the variations caused by altering the parameter's value at the campus level are much more than the ones at the archetype level. For example, the most significant difference between the minimum and maximum DHW flow rates was for the Dormitory with 5.15%. However, since all the buildings were appointed with the Academic Building archetype, the difference between the minimum and maximum DHW flow rates was 35.07% over the entire flow rates in Table 7 In this way, more extensive variations in the parameters' value range catalyzed the detection of their importance on energy consumption. However, more than choosing a single archetype was required to reduce the simulation time.

Eleven parameters were selected for the sensitivity analysis. Simulating two distinct values for each parameter would result in $2,048$ simulations, whereas three parameters denote $177,147$ simulations. Therefore, the sensitivity analysis was divided into two parts. In Sensitivity-1, only each parameter's minimum and maximum values were tested. The aim was to reduce the number of parameters based on their importance in Sensitivity-1 and then examine the remaining parameters in more detail in Sensitivity-2. The minimum, average, and maximum values of the remaining parameters could be tested in Sensitivity-2, which enables the importance of parameters on energy consumption to be observed with a more detailed insight.

Another constraint occurs from the nature of the UMI simulation. UMI creates clusters when dividing buildings into thermal zones in a stochastic manner. This process may result in thermal zones with different amounts of areas or locations on a building's surface. Hence, the cooling and heating consumptions simulated using two identical building templates can differ. Each simulation with a specific template should be repeated until the distribution of the simulation results gets closer to the population mean. Repeating the simulations with multiple cycles could reduce the variations in the simulation results. A single cycle makes $2,048$ simulations with only two distinct values per parameter. Four cycles were conducted considering the computational capacity and time, which made 8,192 simulations. Table 8 shows the details of Sensitivity-1.

The energy consumptions obtained from the simulation of scenarios were analyzed. Each parameter affects energy consumption distinctively. For instance, the cooling set points are likely to affect only the cooling energy consumption, whereas the heating set point only affects the heating energy consumption. Equipment use can affect heating and cooling energy consumption since they fluctuate a building zone's internal heat gains. Reading the effect of a parameter from the total energy consumption might be misleading. Thus, three target consumptions were considered in the sensitivity analysis: (1) Natural Gas, (2) Electricity, and (3) Total Operational Energy. To that end, heating and DHW use were grouped under natural gas consumption, whereas cooling, equipment, and lighting were grouped under electricity consumption.

A linear regression model evaluated each parameter's contribution to these three targets. Linear regression models aim to find the coefficient of the input parameters by looking at their influence on the target variable. If we train a linear model with n parameters according to the targets, which are the energy simulation results, then the model can predict the target using Equation 14:

$$y = a_0 + a_1x_1 + a_2x_2 + \ldots + a_nx_n \tag{14}$$

Table 8 : Sensitivity-1 details

Selected Parameter	Unit	UMI Template Category	Minimum	Maximum
Ground U-Value	W/m2/K	Opaque Constructions	0.304	1.739
Scheduled Ventilation ACH	ACH	Ventilation Settings	0.1	1.0
Infiltration	ACH	Ventilation Settings	0.1	0.5
Heating Set Point	Degree Celsius	Zone Conditionings	20	23
Cooling Set Point	Degree Celsius	Zone Conditionings	23	26
Heating COP	%	Zone Conditionings	80	95
Cooling COP	-	Zone Conditionings	4.5	5.5
EPD	W/m2	Zone Loads	5	15
LPD	W/m2	Zone Loads	5	15
Occupant Density	people/m2	Zone Loads	0.013	0.103
DHW Peak Flow Rate	m3/h/m2	DHW Settings	1.58E-05	7.09E-04

In Equation 15, a_0 is the intercept that represents the bias in the formula, where a_1 to a_n stand for the coefficients of the parameters. These coefficients were scaled between zero and one to compare the importance of features better. This is called relative feature importance. Another metric used in the sensitivity analysis is the Pearson Correlation Coefficient provided in Equation 15 [81]:

$$\mathrm{corr}_x = \frac{\sum_{i=1}^{N}(x_i-\bar{x})(y_i-\bar{y})}{\sqrt{\sum_{i=1}^{N}(x_i-\bar{x})^2\sum_{i=1}^{N}(y_i-\bar{y})^2}} \tag{15}$$

In Equation 15, the term $corr_x$ indicates the correlation between the target y and parameter x, $\bar{x}$ and $\bar{y}$ represent the parameter and target means, and N is the number of scenarios, which is $2,048$ per cycle. Each parameter's relative importance and correlation coefficient were calculated for three targets. Table 9 shows the result of Sensitivity-1 regarding the natural gas consumption.

Table 9 : Sensitivity-1 results based on Natural Gas

Feature Name	Relative Importance	Correlation
DHW Flow Rate	0.333	0.683
Heating Set Point	0.305	0.626
Infiltration	0.119	0.243
EPD	0.076	0.156
LPD	0.074	0.151
Heating COP	0.039	0.080
Occupant Density	0.033	0.068
Ground U-Value	0.012	0.025
Scheduled Ventilation ACH	0.010	0.020
Cooling COP	0.000	0.001
Cooling Set Point	0.000	0.001

The first five parameters correlate more than 10% with natural gas consumption (Table 9). The remaining parameters were less critical in terms of natural gas consumption. DHW flow rate and heating set points were expected to be highly important in natural gas consumption. EPD and LPD, on the other hand, appeared to be the following vital features in natural gas consumption, even though they are supplied by electricity. However, EPD and LPD can be critical in natural gas consumption since they can alter the heat gains of a building zone.

The next target was electricity. It is seen from Table 10 that the EPD and

LPD are the only parameters affecting the electricity consumption with more than 70% correlation each. The other parameters have either a minor or no influence on electricity consumption. When looking at the total operational energy results, there is a mixed order of the important features of natural gas and electricity. The relative importance values in Table 11 suggest that the DHW flow rate, heating set point, LPD, EPD, and infiltration rate comprise almost 90% of the total relative importance. This indicates that the remaining features have a minimal effect on the target variable. However, the occupant density with more than 7% correlation should not be eliminated because it might affect the internal heat gains in building zones. Additionally, occupant density has a 60% CV value in the uncertainty analysis Table 6, and it should be examined in more detail.

Table 10 : Sensitivity-1 results based on Electricity

Feature Name	Relative Importance	Correlation
EPD	0.456	0.706
LPD	0.454	0.703
Cooling Set Point	0.042	0.065
Cooling COP	0.020	0.032
Occupant Density	0.014	0.022
Ground U-Value	0.008	0.013
Infiltration	0.004	0.006
Heating COP	0.001	0.001
DHW Flow Rate	0.001	0.001
Heating Set Point	0.000	0.000
Scheduled Ventilation ACH	0.000	0.000

The first six important parameters from Table 11 were selected for the Sensitivity-2. Plus, the cooling set point, having a 6.5% correlation with the electricity consumption (Table 10), was intuitively selected for the next sensitivity analysis since no parameters directly represented the cooling energy consumption. In the second part of the sensitivity analysis, three values, minimum, average, and maximum, of the selected parameters were investigated once more based on the natural gas, electricity, and total operational energy consumptions. There were $2,187$ scenarios per cycle in Sensitivity-2. This makes a total of 8,748 scenarios from four cycles. Sensitivity-2 was to investigate the influence of the variations in a parameter on energy consumption. Also, it forms a validation step for the Sensitivity-1. The natural gas results in Sensitivity-2 are given in Table 12.

Table 11 : Sensitivity-1 results based on Total Operational Energy

Feature Name	Relative Importance	Correlation
DHW Flow Rate	0.255	0.595
Heating Set Point	0.234	0.545
LPD	0.159	0.371
EPD	0.159	0.369
Infiltration	0.089	0.208
Occupant Density	0.032	0.074
Heating COP	0.030	0.069
Cooling Set Point	0.020	0.046
Cooling COP	0.009	0.022
Scheduled Ventilation ACH	0.007	0.017
Ground U-Value	0.006	0.013

Table 12 : Sensitivity-2 results based on Natural Gas

Feature Name	Relative Importance	Correlation
DHW Flow Rate	0.381	0.712
Heating Set Point	0.309	0.578
Infiltration	0.121	0.226
EPD	0.080	0.149
LPD	0.076	0.142
Occupant Density	0.034	0.063
Cooling Set Point	0.000	0.000

The features' correlations with the natural gas in Table 12 resemble the results of Sensitivity-1 (Table 9). According to this, DHW flow rate, heating set point, infiltration rate, EPD, and LPD appeared to be the most significant features of natural gas consumption. The fact that the DHW flow rate and heating set point stand out in natural gas consumption indicates that the UMI simulation works reasonably. Likewise, infiltration significantly affects the heating energy consumption of the buildings, which is supplied by natural gas, as it can drastically alter the indoor air temperature. EPD and LPD can also be the keys to natural gas consumption because these parameters can affect a building's heating and cooling demand as they cause deviations in the internal heat gains.

Table 13 : Sensitivity-2 results based on Electricity

Feature Name	Relative Importance	Correlation
EPD	0.470	0.707
LPD	0.468	0.703
Cooling Set Point	0.044	0.066
Occupant Density	0.014	0.020
Infiltration	0.004	0.007
Heating Set Point	0.000	0.000
DHW Flow Rate	0.000	0.000

Table 13 illustrates the importance of the features on electricity consumption. These results are similar to the ones in the Sensitivty-1 (Table 10). The first two parameters, EPD and LPD, were expected to be among the crucial features affecting electricity consumption. However, the cooling set point was not too important in either Sensitivity-1 or Sensitivity-2. This shows that cooling demand only covers a small portion of the electricity demand of the campus. Thus, it might be a minor consumption title on the total operational energy of the campus. Likewise, it can be seen from Table 14 that the main determinants of the total operational energy consumption are the ones related to the heating, equipment, or lighting demands. Table 14 shows that occupant density and cooling set point have little importance on the total operational energy consumption relative to the other features. Infiltration rate was among the essential features when the target was natural gas and total operational energy consumption. This proves that infiltration rate mainly affects the heating demand of the buildings, which is supplied by natural gas. Also, the first two important features in Table 14, DHW flow rate and heating set point, belong to the natural gas consumption. It is evident from the overall sensitivity results that the heating-related activities shape the energy demand of the campus. In summary, the two-step sensitivity analysis helped detect the important features of the energy consumption of the campus buildings. The selected features, DHW flow rate, heating set point, LPD, EPD, and infiltration rate, will be further investigated in the next section to reduce the uncertainties in the characterization of campus buildings.

Table 14 : Sensitivity-2 results based on Total Operational Energy

Feature Name	Relative Importance	Correlation
DHW Flow Rate	0.293	0.632
Heating Set Point	0.238	0.513
LPD	0.163	0.351
EPD	0.161	0.347
Infiltration	0.091	0.196
Occupant Density	0.032	0.070
Cooling Set Point	0.021	0.045

4.4 Calibrating the dynamic model using Bayesian Optimization

Consecutive sensitivity analyses helped detect the parameters that hold uncertainty and affect the dynamic energy simulation most. The remaining parameters were deterministically assigned to the archetypes. Here, baseline values obtained from the energy audit report were utilized to characterize the archetype parameters deterministically. On the other hand, different parameter values detected as important after the sensitivity analyses should be examined to optimize the simulation results. Thus, a probabilistic approach is needed to characterize these parameters. Table 15 summarizes the characterization type of the archetype parameters.

Probabilistic archetype characterization considers a joint probability distribution per archetype from different ranges of parameters. In this way, different parameter combinations can be assessed, and the interaction between parameters and their influence on the simulation results can be observed. The minimum and maximum values, acquired either from the energy audit report or the ready-to-use UMI templates, were used to define the value ranges. Then, different values within these ranges were selected for analysis in UMI simulation. For example, Table 16 illustrates the selected values per parameter for the academic buildings.

Table 15 : Parameters and corresponding characterization types

Parameter	Characterization Type
Infiltration	Probabilistic
Heating Set Point	Probabilistic
EPD	Probabilistic
LPD	Probabilistic
DHW Peak Flow Rate	Probabilistic
Cooling Set Point	Deterministic
Heating COP	Deterministic
Cooling COP	Deterministic
Occupant Density	Deterministic
Scheduled Ventilation ACH	Deterministic
External Wall U-Value	Deterministic
Roof U-Value	Deterministic
Ground U-Value	Deterministic
Window U-Value	Deterministic

Academic buildings, dormitory, and social building archetypes have 2,000 scenarios, whereas the sports center has 400 scenarios. The sports center's heating set point is fixed since the inside air is always kept around 24. This reduced the number of parameter combinations for the sports center. Each parameter value should be assessed with all possible combinations of the other parameters. This ensures observing the occurrence probability of a particular parameter value within the joint sample space. Each cycle of simulation in the optimization stage has 6,400 simulations. This makes a total of 25,600 simulations from four cycles. The number of possible values was kept simple for each parameter since performing more than 25 thousand simulations requires much time and computational power. The UMI simulations were performed for only the target archetype, while the other buildings in the model were assumed to be shading objects. This assumption reduced the computational time drastically. The simulation results were stored under the natural gas and electricity consumptions per scenario at the monthly resolution because the highest possible resolution was the monthly resolution for the metered data. Cooling, equipment, and lighting consumptions formed the electricity consumption, whereas heating and DHW consumptions determined the natural gas consumption.

Table 16 : Optimization ranges for the parameters of the academic building

Parameter	Baseline Value	Value-1	Value-2	Value-3	Value-4	Value-5
Infiltration	0.30	0.10	0.20	0.30	0.40	0.50
Heating Set Point	21.50	20.00	21.00	22.00	23.00	-
EPD	5.40	5.00	6.25	7.50	8.75	10.00
LPD	9.40	5.00	7.50	10.00	12.50	15.00
DHW Flow Rate	7.02E-05	2.93E-05	5.65E-05	8.38E-05	1.11E-04	-

UMI utilizes building footprints, basically the plan for the building roof, to derive building volumes. However, the floor plans might deviate from each other. Hence, modeling buildings in UMI caused a slight variation in the conditioned building areas. To overcome this problem, the target simulation results were divided into the GFA of the corresponding archetype to have the energy use intensity (EUI) values. This density representing normalized building energy consumption enabled the validation of the UMI simulation against the metered data. The calibration was performed at the annual resolution based on the natural gas and electricity consumptions. The error between the metered data and the simulation results was calculated using MAPE (Equation 4). A maximum of 25% allowable error limit was determined to include the most possible scenarios in the optimization. The scenarios beyond this maximum error limit were less likely to occur. This limit could have been kept smaller to refine the scenarios with only reasonable simulation results. However, some scenarios could still be valuable even though the error is too high. This is because the scenarios are the combinations of parameters, and an extreme parameter value could drastically change the simulation results, causing a huge error. Therefore, a 25% error limit was employed, and a reasonable number of scenarios were included in the sample space to enhance the interpretation of probabilistic results.

There were two approaches to calibrating the parameters of the dynamic model. The first one is the K-Best approach. Scenario errors were calculated separately for the metered electricity and natural gas consumptions. Then, a target was selected, and scenarios were ordered from smallest to largest error. For example, let us assume that the target is a natural gas error, and then the scenarios are ordered based on the natural gas error. Then, the K-Best approach determines the first scenario in which the natural gas and electricity errors are equal or below the maximum allowable error limit of 25%. This scenario is the ideal case according to the K-Best approach. Here, the term K represents the index of the ideal scenario when all the scenarios are sorted from smallest to largest.

The following approach was the Bayesian Optimization. Bayes' formula determines the posterior probability of an event by looking at the prior probability of the event and the likelihood of that event occurring under certain conditions. The maximum allowable error limit of 25% was utilized to label scenarios. According to this, scenarios with less than 25% error for both natural gas and electricity were labeled as Included, whereas the others were labeled as Not Included. The sample space for the Bayesian Optimization covers only the included scenarios. The Bayes formula was defined as in Equation 16 in our case:

$$P(x_i \mid \text{Included}) = \frac{P(\text{Included}|x_i)P(x_i)}{P(\text{Included})} \tag{16}$$

In Equation Equation 16, x_i represents the single value of a parameter. $P(x_i)$ is the prior probability of the value of a parameter. Since the parameters selected for the optimization stage offered no prior knowledge about their distributions, the prior probabilities were modeled as uniform distributions. However, considering the computational constraints, the possible values of a parameter should be finite, which results in a discrete uniform distribution. For example, the possible value range for the infiltration rate of the academic buildings was 0.1 to 0.5. Only five distinct values within this range were considered rather than covering all possible values (Table 16). This suggests that the prior probability of each value is the same and equal to 0.2. The term $P(\text{Included} \mid x_i)$ is called the likelihood, and it represents the conditional probability of the number of included scenarios occurring when a parameter gets the value of x_i. This likelihood constitutes the stochastic structure of the Bayesian Optimization in the study.

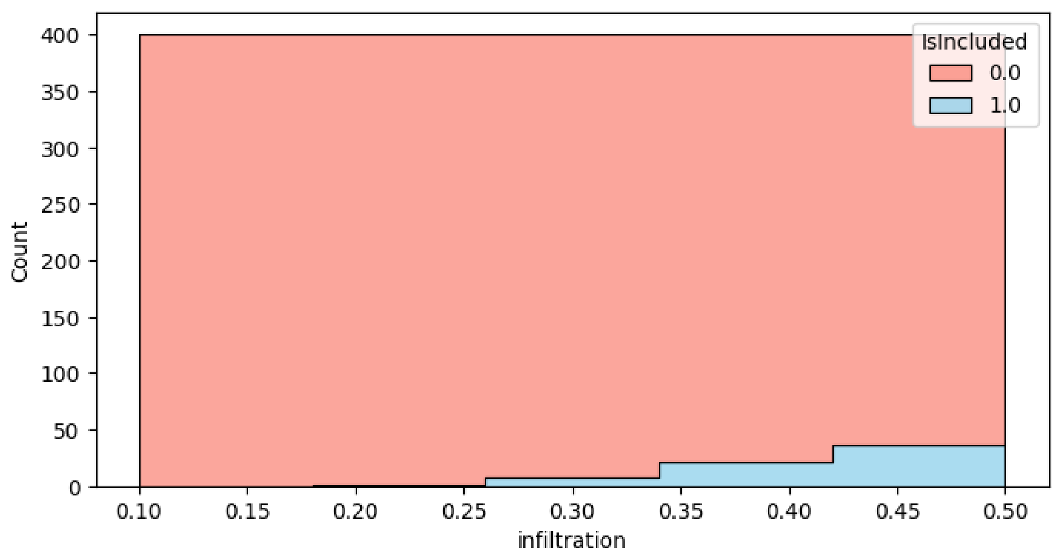

Figure 11 : Likelihoods of the infiltration values for Academic Building

According to Bayesian Optimization, the posterior probability of x_i depends on the number of included scenarios it appears in. Hence, the probability of x_i occurring increases as the number of included scenarios it appears in increases. In other words, x_i is likely to be the optimal value of a parameter as the scenarios it appears in exhibit less and less error based on the natural gas and electricity consumption. For example, the likelihood increases as the infiltration rate increases, as shown in Figure 11. This suggests that the infiltration rate of 0.5 outperformed the other values in taking part in the included scenarios. The comparison of the prior and posterior distributions for this same parameter is illustrated in Figure 12.

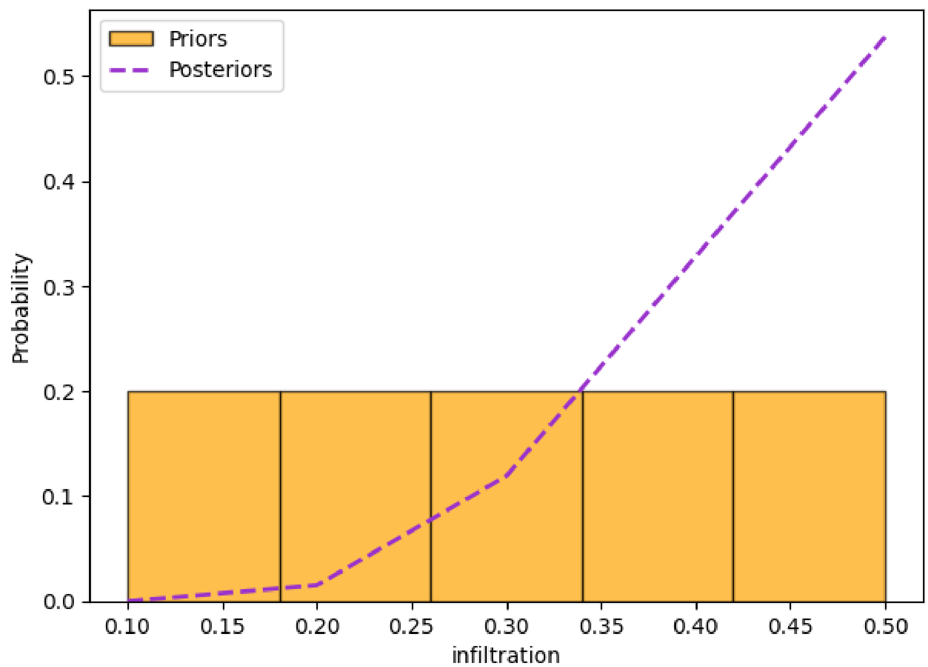

Figure 12 : Prior and posterior distributions of the infiltration for Academic Building

Table 17 : Selected parameters of the Academic Building for different optimization approaches

Approach	DHW Flow Rate	EPD	Heating Set Point	Infiltration	LPD
K-Best	1.11E-04	8.75	23.00	0.30	5.00
Bayesian Optimization	1.11E-04	6.25	23.00	0.50	5.00

Each archetype was evaluated according to the two optimization approaches summarized above. For example, Table 17 provides the parameter combinations of the K-Best and Bayesian approaches for the Academic Building. The only difference is from EPD and infiltration rate based on Table 17. The best parameter combination for each approach was utilized for archetype characterization. In this step, three models were employed in a final comparison. The first model is the baseline model, in which the archetypes were deterministically characterized. The second model was where the archetype was characterized according to the K-Best approach. Lastly, the third model utilized Bayesian Optimization in characterizing the archetype parameters. UMI simulations were performed for each model. The operational energy from the validation data was used to assess the performance of these three models. The MAPE of 13 buildings at the monthly and annual resolutions for these three models are given in Table 18.

Table 18 : Validation data vs. three models based on the monthly and annual MAPEs

Models	Monthly MAPE (%)	Annual MAPE (%)
K-Best	14.84	4.86
Bayesian Optimization	9.90	4.60
Baseline Model	22.14	21.56

It is evident from Table 18 that the calibrated models through different optimization approaches outperformed the baseline model, which was deterministically characterized. The baseline model exhibits 21.56% and 22.14% errors against the metered data at the monthly and annual resolutions. Optimizing the archetype parameters reduces simulation errors. The monthly and annual errors for the K-Best approach were 14.84% and 4.86%, whereas they were 9.90% and 4.60% for the Bayesian Optimization. The Bayesian approach utilized in the study provided the least simulation error according to the validation data. There might be several reasons for this outcome. The K-Best approach deterministically selects the optimal scenario by only looking at the magnitude of the error. However, as said before, a parameter's extreme value might fluctuate the simulation results and cause errors that are too high or too low, while the rest of the parameters in the combination might not yet reach their optimal values. For example, the infiltration rate has a massive effect on the simulation results, and the maximum value of the infiltration rate could yield a small error while the rest of the parameter combination stands at the minimum values. On the other hand, a new interpretation of the Bayesian likelihood proposed in the study evaluates the distribution of the parameter values based on the number of included and not included scenarios. The occurrence probability of a parameter's value was derived from a joint distribution per archetype, in which the interaction between parameters and their resultant effect on energy consumption was analyzed. Thus, it holds insights into the most suitable parameter combinations for the campus buildings' archetypes. In this way, the calibrated model over Bayesian Optimization provided the best simulation results.

CHAPTER V

STATISTICAL MODEL

The calibrated dynamic model using Bayesian Optimization created hourly energy consumption data. Since the monthly error of the calibrated was under 15%, which is a reasonable limit according to a relevant ASHRAE Standard [22], the calibrated model was assumed to be capable of creating hourly energy consumption for the campus buildings. The hourly energy consumption of the campus buildings served as the validation data of the statistical model. Many data-driven models can predict building energy consumption. However, the task was to predict the hourly energy consumption, which is a highly time-dependent work. For example, the energy consumption of a building at a specific time step can be influenced by the energy consumption for the previous time steps. The fluctuations in the weather data from the previous hours can also affect the upcoming consumption. Hence, LSTM was selected as the statistical model in the study. LSTM is a time-series model that analyzes the sequential interaction in data. The predictions are based on the input data in regular feed-forward models, such as a simple MLP. The MLP takes the weighted average of the input set with pre-defined layer weights, transforms them into a non-linear state using the activation function $f(\cdot)$, and provides a prediction for each observation. In a typical feed-forward model, the prediction can be represented as in Equation 17:

$$y_t = f(x_t) \tag{17}$$

In Equation 17, y_t is the prediction over the observed input set x_t at time t. The feed-forward models only investigate the given observation at a time t. Hence, there is no time dependency in such models. LSTM models, on the other hand, store in memory the changes occurring over time and use them in making predictions (Equation 18):

$$y_t = f(x_t, h_{t-1}) \tag{18}$$

As seen from Equation 18, the activation function in the LSTM models included a memory term, h_t. This term allows the LSTM to understand the interaction between inputs and targets from a time perspective. Therefore, LSTM models are called sequential models. The time interval called sequence length that the LSTM model must cover is uncertain and could be determined after intensive trials. For example, the sequence length of three covers the state of the last three hours. This might be helpful when the data does not include long-term patterns, and the targets should be evaluated at small intervals. On the other hand, a sequence length of 24 hours can allow the daily patterns in data to be observed while keeping the hourly patterns. However, as the sequence length increases, the meaning from the small-time intervals starts vanishing, and the models start capturing the long-term patterns. Also, increasing the sequence length complicates the model structure and yields longer training times. Therefore, the sequence length should be selected carefully.

A single LSTM model was created for each building, which makes 13 models in total. The energy audit report provides the building characteristics, such as GFA, envelope properties, HVAC details, and operational schedules. However, since each LSTM model includes only one building, most characteristics are useless in training. For example, let us consider the AB1 building. 8,760 hourly energy consumption was obtained from the UMI simulation using the calibrated model. Some of the input data for AB1, including the U-Value, EPD, LPD, or Heating Set Point, will be static features. This means that these features will be the same for 8,760 observations. The models cannot derive information without variance in the input data. Therefore, all the static features become ineffective. On the other hand, building operational schedules (e.g., heating schedules) and weather data (e.g., temperature) are inputs that change over time. Therefore, the building operational schedules and the weather data formed the primary input source of the LSTM model. The building operational schedules involved the heating, cooling, DHW use, equipment use, lighting use, and occupancy schedules. Meanwhile, the weather data included dry bulb temperature, dew point temperature, relative humidity, wind direction, wind speed, hourly total global solar radiation, sun exposure intensity, and liquid precipitation depth.

However, excluding the static features causes the loss of a massive amount of information since the targets, which are the hourly energy consumption, are shaped by the building characteristics. To that end, the building operational schedules and weather data were combined with the building characteristics. For example, a new feature called Equipment Load Density. The EPD density obtained from the calibrated model was multiplied by the hourly equipment use schedules. This provided an EPD changing over time. The same procedure was repeated for the LPD, DHW Flow Rate, and Occupant Density by utilizing their operational schedules.

Additionally, the heating and cooling set points were made functional with the aid of the hourly weather data and the operational schedules for zone heating and cooling. During a chosen hour, if a zone conditioning schedule is active, indicating that the observed hour is in the operational time, and the outside air temperature is either above or below the setpoint, meaning that the zone requires conditioning, then two new features, namely Heating Requirements and Cooling Requirement, represent the difference between the outside air temperature and the conditioning set point. In this way, the heating and cooling setpoints, which are static features, were transformed into features that change over time.

$$x_{\text{scaled}} = \frac{x - x_{\min}}{x_{\max} - x_{\min}} \tag{19}$$

The architecture of LSTM models can be complex. They consist of many hyperparameters that can massively affect the prediction quality. The first hyperparameter is the method of normalization. All features should be within similar ranges to enhance the quality of model training. Normalization could be performed using different techniques, such as minimum to maximum scaling within a specific range (Equation 19), or standard scaling, which is the Z-Score Normalization, based on the mean and standard deviation of the feature (Equation 20). In Equation 20, μ represents the mean of the feature, whereas σ represents the standard deviation of the feature.

$$Z = \frac{x-\mu}{\sigma} \tag{20}$$

Another hyperparameter is the sequence length. Sequence length in an LSTM model determines the temporal homogeneity the model seeks for patterns. As the sequence length gets longer, the focus of the patterns is transformed from smaller intervals (e.g., hourly) to higher intervals (e.g., monthly). The next hyperparameter is the batch size. Batch size is the number of training examples observed in a single iteration. The batch size can massively affect the performance of model training as larger batch sizes can lead to faster training but may require more memory, while smaller batch sizes may provide more accurate error reduction but could slow down the training phase. The number of hidden layers and hidden units are the essential hyperparameters of every neural network, including the LSTM model, which is a version of RNNs. Hidden layers and hidden units determine the complexity of the model architecture, and they should be tested elaborately. Neural network models adapt an online learning process by separately observing the instances of a dataset [23]. This process is called Online Learning, in which the model updates its weights according to the given instance. The update happens based on the gradient of the error calculated between the target and the prediction. The gradients are the partial derivates of the error function according to the model weights. The final update is found by multiplying the gradient by the learning rate. The error function is another hyperparameter. It depends on whether the task is regression or classification. In our case, hourly energy predictions are continuous values. Thus, the task is regression. The most popular error (loss) functions are the Mean Square Error and the Mean Absolute Error. The selected loss function can notably influence the error measured between the targets and predictions. Hence, it directly affects the learning process of the model. This brings us to the next hyperparameter called learning rate. The learning rate controls the pace of the updates during the optimization of the model weights. Choosing an optimal learning rate is vital since the learning rate affects the accuracy and the speed of the convergence in model training. The learning rate should be examined with another hyperparameter called epoch. The number of epochs indicates the complete cycle time in which the model processes each instance and learns from them during the training phase. Within a single epoch, the model examines all the data in batches, calculates errors, and updates the model's weights based on the specified batch size. Once all the instances are evaluated, one epoch is then considered complete.

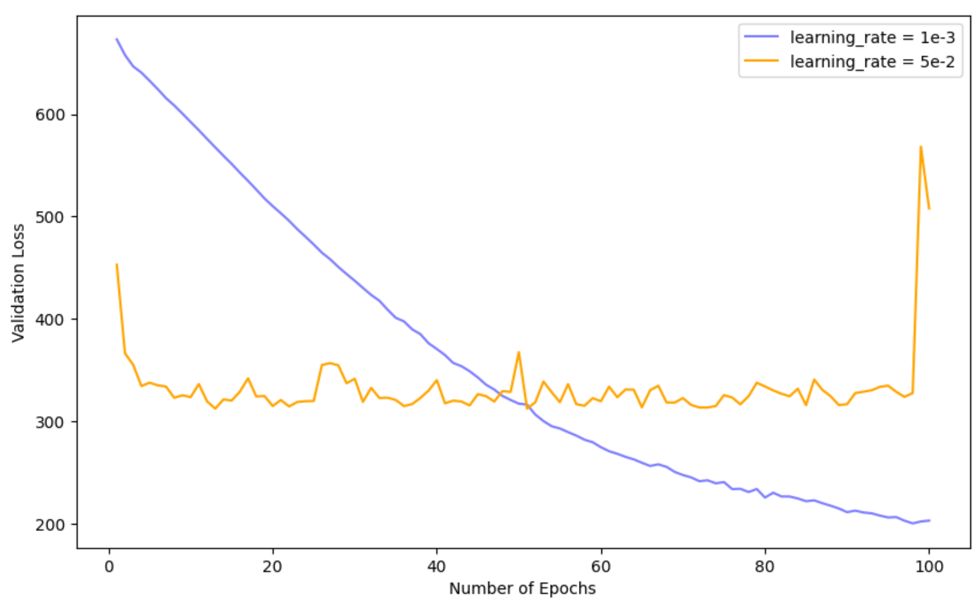

Figure 13 : Comparison of learning rates

The connection between the learning rate and the number of epochs is illustrated in Figure 13. The models here were trained using different learning rates, and their performance was assessed over the validation data using the same number of epochs. The higher learning rate of 0.05 exhibits significant fluctuations. This model could not converge since the updates are excessive, and the model cannot be effectively trained. Conversely, the small learning rate of 0.001 requires additional training epochs to minimize the validation loss as it underfits the training data. Figure 13 underlines the importance of simultaneously and judiciously selecting the learning rate and number of epochs for optimal model training.

Table 19 : Optimal hyperparameter setting according to the AB1 model

Hyperparameter	Value
Normalization	Standard Scaler
Sequence Lenth	6 (hours)
Batch Size	24
Number of Hidden Layers	2
Number of Hidden Units	54
Error (Loss) Function	Mean Absolute Error
Learning Rate	1e-3
Number of Epochs	200

The hyperparameter tuning was performed over the AB1 building. The combinations of the hyperparameters mentioned above were tested using the AB1 building. There were 960 parameter combinations in total. The input data was split into training, validation, and test sets. This is a standard application in machine learning. The training set has 80% of the observations, whereas the validation and test sets have 10% each. The training set was used to train the model and find the optimal weights. Then, the performance of the trained models was assessed over validation data. The scenario that gives the minimum validation error was selected. The error metric was the R-squared value. The optimal hyperparameter setting from the selected scenario is summarized in Table 19.

The validation curve in Figure 14 summarizes the parameter tuning process based on the learning rate and the number of epochs. In the validation curve, the continuous red represents the training loss, whereas the dashed blue line represents the validation loss. Notably, the slope of the validation loss diminishes as the number of epochs increases. After 150 epochs, the validation loss stays the same. In contrast, the training loss consistently decreases with the growing number of epochs. This is because the model learns more and more from the training data and starts overfitting. Consequently, this might cause the trained model to lose its generalization capacity and the reduction of the validation loss to be either stopped or reversed.

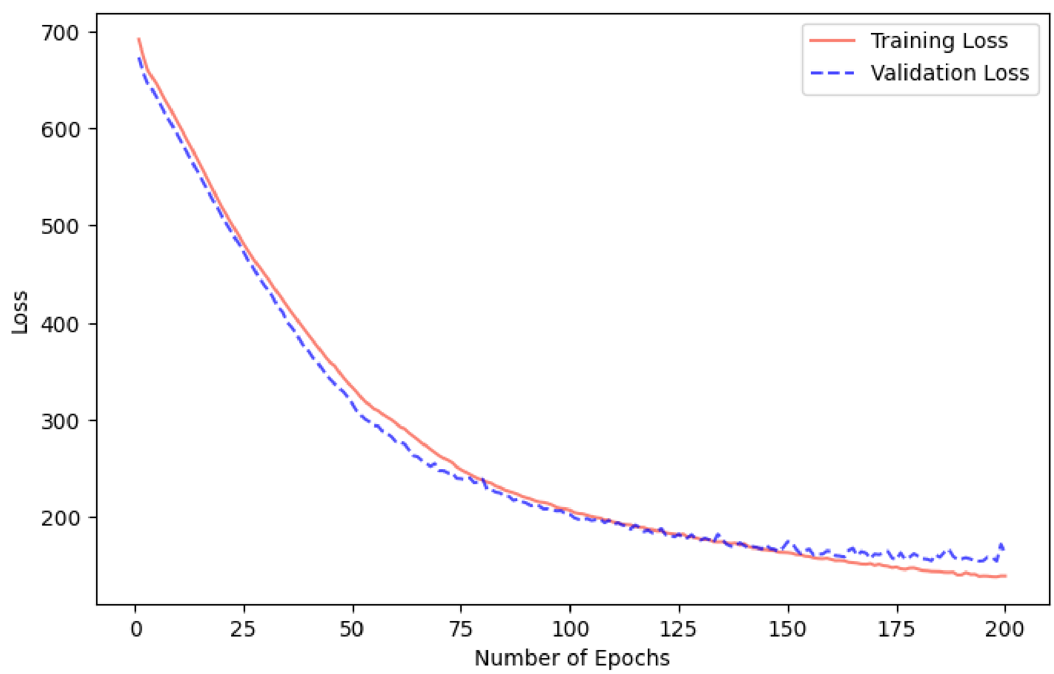

Figure 14 : Validation curve for AB1

The optimal hyperparameter setting from Table 19 was utilized to analyze the performance of the 13 LSTM models over their test sets. The performance of the LSTM models is illustrated in Table 20. Overall, the regression results of the LSTM models are promising. The LSTM models of dormitory buildings and the sports center outperformed the other models. Average R-squared values for the academic buildings are 0.839, whereas the average R-squared value for dormitories is 0.993. This is followed by an average of 0.830 and 0.916 for the social building and sports center.

Table 20 : Evaluation of the hourly energy consumption predictions over the test sets

LSTM ID	Test - R2 Score	Test - MAE	Test - MSE
AB1	0.841	166.91	131,558.81
AB2	0.848	137.24	80,394.76
AB3	0.836	69.62	43,968.43
AB4	0.822	212.50	194,041.23
SCOLA	0.849	58.71	34,807.25
OM	0.830	109.73	85,764.90
SM	0.916	27.62	7,960.05
Y1	0.997	8.51	250.48
Y2	0.997	6.09	150.74
Y3	0.993	7.48	295.18
Y4/5	0.991	31.66	3,490.99
Y6	0.982	41.77	6,742.15
GH	0.996	3.71	52.26

The hyperparameter tuning was performed over AB1, which is an academic building. However, the dormitory buildings employed the optimal hyperparameter combination in the best way to provide accurate regression results. Nevertheless, the input data for different buildings have similar structures with all non-static features based on the operational schedules. Therefore, the regression results are reasonable. Another reason for the high accuracy of the dormitory models is that there might be more minor variations in the characteristics of the buildings included in the Dormitory archetype. Notably, the proposed LSTM models were equipped only with the non-static features from the building operational schedule and weather data. Integrating the building characteristics, such as envelope properties and HVAC details, can enormously increase the regression performance. However, such static features require different algorithm approaches when developing time-series models. Overall, the LSTM models yielded an average of 0.915 R-squared in predicting the hourly energy consumptions.

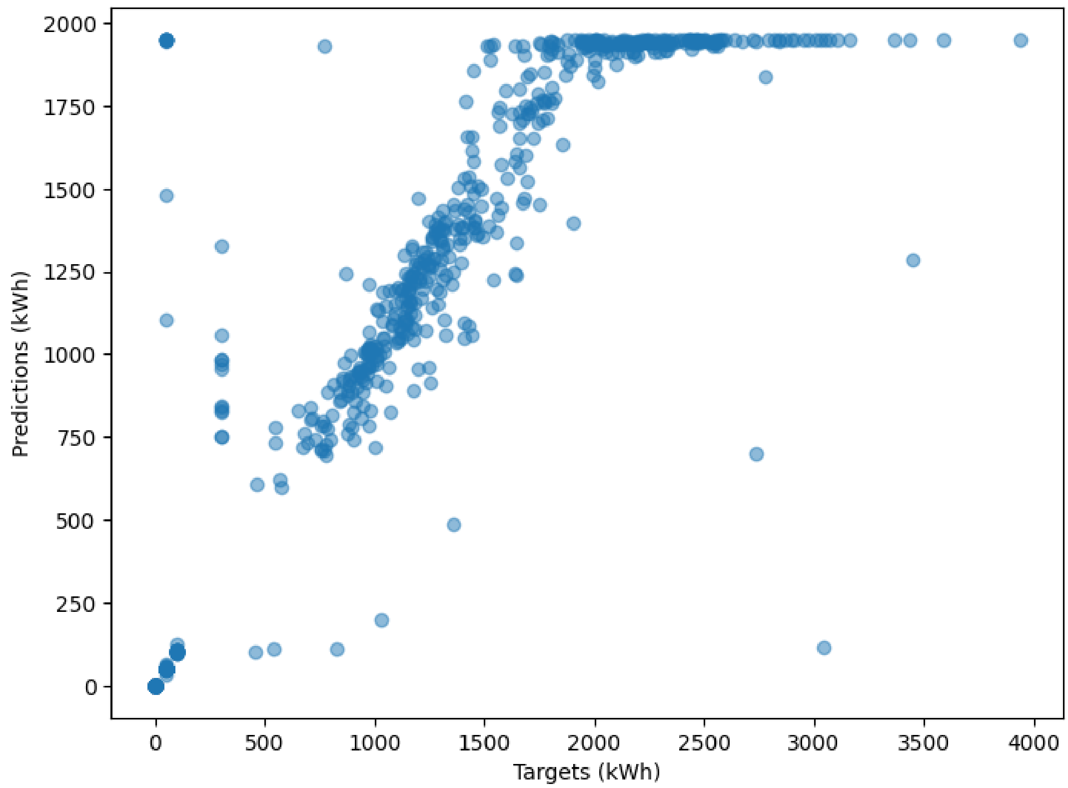

Figure 15 : Hourly energy consumption predictions of the AB1 model

Figure 15 shows the predictions of the AB1 model compared to the targets. The AB1 model performed well in predicting the target consumptions between 0 and $2000kWh$, whereas it could not reflect the consumptions with more than $2000kWh$. The evaluation of the LSTM models equipped only with the non-static feature set at the hourly resolution proved that there is still room for improvement. The performance of the LSTM models was further investigated against the validation data. Table 21 summarizes the average monthly errors of the LSTM models against the metered data. The weight of the trained models was then utilized to make predictions at the annual resolution. This provided 8,760 predictions per model. Then, these predictions were cumulated under the monthly consumptions and divided into the GFA of the corresponding building to derive the EUI values. Finally, the monthly

EUI values were compared against the metered data (Table 22).

Table 21 : Evaluations of EUI predictions at the monthly resolution over the entire data

LSTM Model	MAPE
AB1	0.297
AB2	0.278
AB3	0.105
AB4	0.289
SCOLA	0.135
OM	0.138
SM	0.124
Y1	0.221
Y2	0.253
Y3	0.267
Y4/5	0.451
Y6	0.255
GH	0.295

Table 22 : Performance comparison of the dynamic and statistical models against the metered data

Model	Monthly MAPE (%)
Dynamic Model (calibrated)	9.90
Statistical Model (LSTM)	23.91

According to Table 22, the LSTM models predicted the monthly energy consumption of the campus buildings with a 21.91% MAPE, whereas the dynamic model, which was calibrated using Bayesian Optimization, simulated the monthly consumptions with a 9.90% MAPE. These results are understandable since the statistical models were built on the simulation results of the dynamic model. Therefore, they were expected to exhibit more considerable errors than the dynamic model. The performance of the LSTM models depends on the simulation quality. If the simulation results can better represent the validation data, the hourly energy predictions of the LSTM models can be improved.

CHAPTER VI

DISCUSSION

There are examples of studies integrating dynamic and statistical models in UBEM. However, these studies either lack parameter calibration and model validation [17], provide predictions at a low temporal resolution [16], or need to utilize a proper dynamic model [19]. Thus, there is a need for a novel hybrid approach in UBEM. In this sense, this study developed a hybrid approach by integrating the substantial elements of different modeling techniques in UBEM. First, a calibrated dynamic model created consistent synthetic hourly energy consumption data in this sense. The synthetic data then formed the statistical models' validation data. The statistical model performed a time-series analysis and reasonably predicted the hourly energy consumption of the buildings. The proposed approach showed that hybrid modeling techniques can be valuable in UBEM. A simple but powerful approach in Bayesian Optimization provided the most suitable parameter combination rather than deterministically selecting the combination with the least simulation error. Such model calibration can be valuable in creating synthetic data for studies without hourly validation data. Transforming non-static features of the buildings into time-dependent features by utilizing the building operational schedules proved the importance of occupant-related parameters in UBEM. Plus, this study emphasized the value of feature extraction in machine learning based on the solid performance of the LSTM models in predicting hourly energy consumption.

Within the scope of this study, the proposed hybrid model can optimize the building's energy efficiency design by exploring various configurations in the building envelope and operational details and minimizing energy consumption and the resultant environmental impact. For example, different values for the building insulation or various scenarios on the zone conditioning scenarios can be tested over the proposed model, and these results can identify the necessary action to reduce energy consumption. Likewise, the impact of climate change on the observed area can be foreseen and mitigated as the proposed model can utilize the weather data effectively. Moreover, the proposed hybrid model can evaluate the energy reduction strategies at the urban level. Hourly synthetic energy consumption data enable understanding of the deviations in the building energy consumption patterns within higher resolution. These patterns can be combined with the building characteristics, and the determinant parameters shaping the building energy demand can be extracted. In addition, the proposed hybrid UBEM can guide urban planners in detecting districts with high energy demands and generating energy-efficient interventions for urban building stocks. Such observation and control power allow urban planners to identify areas where energy resources are under significant pressure or where potential inefficiencies occur. Urban planners can also evaluate the potential return on investment for implementing energy-efficient measures in specific areas by utilizing the proposed hybrid model. All the mentioned energy reduction and cost-effectiveness scenarios at the campus and urban levels can be tested instrumentally using the statistical model. The statistical model was partially equipped with the optimized parameters of the dynamic model. Therefore, the statistical model has the potential to estimate buildings' energy consumption at the hourly resolution accurately as its feature set contains the ideal parameter combination of the dynamic model that gives the least simulation error against the metered data. However, there are some limitations that this study must overcome.

The trigeneration effect and the excluded seasons (e.g., pandemic period) complicated utilizing the metered data from more extended periods and understanding long-term patterns in the building's energy consumption Figure 10. Also, the final validation data derived from the processed metered data includes many assumptions within measuring the trigeneration effect, such as the system efficiency, waste energy distribution per season, and baseline heating demand for the summer. These assumptions and actions may have reduced the reliability of the data. Most of the simulation parameters were obtained from the energy audit report. However, some parameters, such as infiltration rate and EPD, remained uncertain. Even though these parameters were optimized within a reliable range, there were no prior thoughts about their distribution. Therefore, they were modeled as uniform distribution, and the effect of the prior probability in Bayesian Optimization became ineffective. The air tightness and equipment/lighting use of a building zone can be examined using sensors. This might help to derive prior information about the parameters and reduce the uncertainty in archetype characterization.

Building characterization was performed over the selected archetypes by using the average parameter values of the buildings obtained from the energy audit report. Although there was little or no uncertainty for those values, the generalization process within the archetype might have caused a loss of information. Like the unknown parameters, the averaged archetype parameters can be calibrated so the archetypes can better represent the building within them. Another important parameter was the building operational schedules. These schedules were derived using the energy audit report, the information from the university officials, and ready-to-use UMI templates. However, the archetype characterization only focused on the static parameters (e.g., heating set Point), keeping the time-dependent parameters simple (e.g., heating schedule). Monitoring the occupant-related activities can be an excellent solution to derive more elaborate operational schedules. For example, the number of occupants and operational schedules can be estimated by recording entrances and exits to the campus. The calibration of the dynamic model was performed according to the annual natural gas and electricity consumptions. This enabled obtaining general energy consumption patterns of the building across a whole year. However, the correlation between the simulation parameters and the simulation results should be investigated in more detail than the annual resolution. This is because distinct seasons of a year, even different weeks of a month, could cause massive variations in the parameter values that give the most accurate simulation results. A possible future work can be dividing the optimization into monthly chapters and deciding on the ideal parameter combination by looking at the simulation error of these chapters.

The following limitation emerged in the statistical model. Hyperparameter tuning was performed over the AB1 buildings. The training and validation set of the input data of AB1 were analyzed, and the optimal hyperparameter combination was attained. This combination was then utilized to train all the LSTM models and make predictions accordingly. The computational constraints in the study did not allow comprehensive hyperparameter tuning (Table 23). However, buildings differ in terms of characteristics and operational patterns. Nevertheless, considering the urban context with many buildings, tuning the hyperparameters of the LSTM model of each building is not practical. A possible solution lies in the archetype approach. Each archetype should be subjected to individual hyperparameter tuning so the LSTM models can more effectively perform predictions.

Table 23 : Work packages and corresponding simulation times

Work Package	Model Involved	Number of Scenarios	Computation Time (hours)
Sensitivity-1	Dynamic Model	8192	113.8
Sensitivity-2	Dynamic Model	8748	121.5
Optimization	Dynamic Model	25600	142.2
Hyperparameter Tuning of LSTM	Statistical Model	14400	32.0

Table 23 summarizes the computational time of each working package of the study. The dynamic energy simulation and training of RNN models demand a great time.

Determining the optimal dynamic and statistical models took more than 17 days. According to Table 23, the dynamic model evaluated around 113 scenarios in an hour, whereas the statistical model examined 450 scenarios per hour. Table 23 demonstrates the speed and effectiveness of statistical models in analyzing building energy performance while highlighting our motivation in creating a hybrid model. It should be noted that all the simulations and predictions were performed using a single workstation. The computational time can be reduced by parallel processing with several computers.

This study can benefit urban planning when the mentioned limitations are addressed. The proposed methodology offers the potential to identify and optimize unknown parameters using a probabilistic approach. This is particularly valuable at the urban scale, where building characterization is challenging due to the requirement for accurate input data. Building inspection surveys, building energy audit reports, building energy standards, and municipal data sources can help derive building archetypes and characterize them with energy-related parameters, such as building envelope properties and operational schedules.

Time-dependent features were utilized in creating individual LSTM models, while static features, such as WWR, infiltration rate, and occupant density, were discarded. A joint LSTM model, integrating the input data of all 13 buildings, can utilize the static features left behind. Each building will have its building characteristics in the joint model. Therefore, static feature columns will exhibit variations and be valuable in the joint model. Thermal interaction between the campus buildings is another question to consider in future works. Besides the static features from the building characteristics and the time-dependent features, such as building operational schedules and weather data, the location and the three-dimensional interaction between the campus buildings can be valuable. For example, the surrounding buildings can influence solar radiation on a building's surface. Likewise, the wind effect in outdoor corridors formed by building settlement causes significant changes in the temperature of the building facades. New features can be created to enhance the prediction capacity of the statistical model considering the thermal interaction between buildings. For instance, a location feature can be added to the statistical model that holds insights into the building's latitude, longitude, and altitude. Another future research direction could be developing an automated decision tool to evaluate scenarios and achieve energy reduction, such as modifying building envelope properties or operational schedules. This tool can accurately predict the impact of any alteration in building characteristics by appropriately incorporating the energy-related parameters of the buildings and climate conditions within the statistical model.

CHAPTER VII

CONCLUSIONS

This study bridges a critical research gap in UBEM by introducing a novel hybrid approach that integrates dynamic and statistical models. The existing literature reveals that prior studies either lack parameter calibration and validation, provide predictions at a low temporal resolution, or neglect the utilization of a proper dynamic model. Thus, the need for an innovative hybrid approach became evident. Accurately monitoring hourly energy consumption in buildings is essential for understanding patterns and uncertainties in energy use. While statistical models face challenges in accurately predicting hourly energy usage, dynamic models, while effective, are complex, requiring detailed data and time. Additionally, since the metered data is only at the monthly resolution, a robust dynamic model was necessary to replicate the hourly consumption of the building. All these considerations led us to develop an innovative hybrid UBEM.

To that end, an integrated UBEM was created for time-series analysis in this study. The approach was started by creating a dynamic model for 13 buildings on the Özyeğin University campus. The critical parameters of the dynamic model were detected and calibrated using Bayesian Optimization. The optimization was performed based on natural gas and electricity uses at the annual resolution. According to the metered data, the MAPE for the simulation results of the baseline model was reduced from 21.56% to 4.60% at the annual resolution and from 22.14% to 9.90% at the monthly resolution, thanks to model calibration. The hourly energy consumptions created by the simulation of the calibrated model were then utilized in the statistical model. The statistical model comprises a time-series analysis with LSTM. 13 LSTM models per building were created and equipped with time-dependent features. The hourly energy predictions over the test sets provided an average of 0.915 R-squared value. The LSTM models were employed to predict hourly energy consumption for a year. These predictions were then clustered into monthly predictions to be compared with the metered data since the metered data was available at the monthly resolution. Here, the LSTM models exhibited an average of 21.91% MAPE.

This study facilitates energy-efficient building design on the Özyeğin University campus by exploring diverse building configurations (e.g., testing different insulation values) and operational details (e.g., altering zone conditioning options). Notably, the applicability of the proposed hybrid model can be extended to the urban scale, where urban planners can identify high-energy-demand areas, propose efficient interventions, and assess potential returns on investment by utilizing the hourly energy consumption predictions of the hybrid model. The proposed hybrid model's capabilities are due to its efficiency in observing and controlling the energy use of the building stocks via time-series analysis. After optimizing a dynamic model, the proposed hybrid model can equip a site's building characteristics and weather details. Thus, it can accurately monitor the hourly building's energy use and reasonably offer energy reduction strategies. The final output of the hybrid model, obtained from the statistical model, makes time-series analysis effective and robust. Therefore, this study highlights the potential of hybrid modeling in UBEM and offers valuable insights for future applications.

REFERENCES

[1] T. Dogan and C. Reinhart, "Shoeboxer: An algorithm for abstracted rapid multi-zone urban building energy model generation and simulation," *Energy and Buildings*, vol. 140, pp. 140–153, 4 2017.

[2] Y. Jia, A. Anaissi, and B. Suleiman, "ResNLS: An improved model for stock price forecasting," *Computational Intelligence*, 11 2023.

[3] OECD, *CO2 Emissions in 2022*. 2023.

[4] O. G. Santin, L. Itard, and H. Visscher, "The effect of occupancy and building characteristics on energy use for space and water heating in Dutch residential stock," *Energy and Buildings*, vol. 41, pp. 1223–1232, 11 2009.

[5] A. Oraiopoulos and B. Howard, "On the accuracy of Urban Building Energy Modelling," *Renewable Sustainable Energy Reviews*, vol. 158, p. 111976, 4 2022.

[6] C. Reinhart and C. C. Davila, "Urban building energy modeling – A review of a nascent field," *Building and Environment*, vol. 97, pp. 196–202, 2 2016.

[7] M. Ferrando, F. Causone, T. Hong, and Y. Chen, "Urban building energy modeling (UBEM) tools: A state-of-the-art review of bottom-up physics-based approaches," *Sustainable Cities and Society*, vol. 62, p. 102408, 11 2020.

[8] D. Wang, J. Landolt, G. Mavromatidis, K. Orehounig, and J. Carmeliet, "CESAR: A bottom-up building stock modelling tool for Switzerland to address sustainable energy transformation strategies," *Energy and Buildings*, vol. 169, pp. 9–26, 6 2018.

[9] N. Buckley, G. Mills, C. Reinhart, and Z. Berzolla, "Using urban building energy modelling (UBEM) to support the new European Union's Green Deal: Case study of Dublin Ireland," *Energy and Buildings*, vol. 247, p. 111115, 9 2021.

[10] L. G. Swan and V. I. Ugursal, "Modeling of end-use energy consumption in the residential sector: A review of modeling techniques," *Renewable Sustainable Energy Reviews*, vol. 13, pp. 1819–1835, 10 2009.

[11] T. Hong, Y. Chen, X. Luo, N. Luo, and S. H. Lee, "Ten questions on urban building energy modeling," *Building and Environment*, vol. 168, p. 106508, 1 2020.

[12] S. Fathi, R. Srinivasan, A. E. Fenner, and S. Fathi, "Machine learning applications in urban building energy performance forecasting: A systematic review," *Renewable Sustainable Energy Reviews*, vol. 133, p. 110287, 11 2020.

[13] A. Booth, R. Choudhary, and D. Spiegelhalter, "Handling uncertainty in housing stock models," *Building and Environment*, vol. 48, pp. 35–47, 2 2012.

[14] H. Kazmi, C. Fu, and C. Miller, "Ten questions concerning data-driven modelling and forecasting of operational energy demand at building and urban scale," *Building and Environment*, vol. 239, p. 110407, 7 2023.

[15] Y. Q. Ang, Z. Berzolla, and C. Reinhart, "From concept to application: A review of use cases in urban building energy modeling," *Applied Energy*, vol. 279, p. 115738, 12 2020.

[16] C. Y. Yi and C. Peng, "An archetype-in-neighbourhood framework for modelling cooling energy demand of a city's housing stock," *Energy and Buildings*, vol. 196, pp. 30–45, 8 2019.

[17] U. Ali, S. Bano, M. H. Shamsi, D. Sood, C. Hoare, W. Zuo, N. Hewitt, and J. O'Donnell, "Urban building energy performance Prediction and retrofit Analysis using Data-Driven Machine Learning approach," *Energy and Buildings*, vol. 303, p. 113768, 1 2024.

[18] M. Brøgger, P. Bacher, and K. B. Wittchen, "A hybrid modelling method for improving estimates of the average energy-saving potential of a building stock," *Energy and Buildings*, vol. 199, pp. 287–296, 9 2019.

[19] J. Roth, A. Martin, C. Miller, and R. K. Jain, "SynCity: Using open data to create a synthetic city of hourly building energy estimates by integrating data-driven and physics-based methods," *Applied Energy*, vol. 280, p. 115981, 12 2020.

[20] R. McNeel and Associates, *Rhinoceros: Nurbs Modeling for Windows.* Robert McNeel and Associates, 2008.

[21] D. B. Crawley, L. K. Lawrie, F. Winkelmann, W. Buhl, Y. Huang, C. Pedersen, R. K. Strand, R. J. Liesen, D. E. Fisher, M. J. Witte, and J. Glazer, "EnergyPlus: creating a new-generation building energy simulation program," *Energy and Buildings*, vol. 33, pp. 319–331, 4 2001.

[22] A. G. ASHRAE, "Guideline 14-2002: Measurement of energy and demand savings," *ASHRAE, Atlanta*, 2002.

[23] E. Alpaydin, *Introduction to Machine Learning, fourth edition.* MIT Press, 3 2020.

[24] J. Schmidhuber, "Deep learning in neural networks: An overview," *Neural Networks*, vol. 61, pp. 85–117, 1 2015.

[25] S. Hochreiter, "Untersuchungen zu dynamischen neuronalen netzen," 1991.

[26] K. He, X. Zhang, S. Ren, and J. Sun, "Deep residual learning for image recognition," *arXiv (Cornell University)*, 12 2015.

[27] S. Hochreiter and J. Schmidhuber, "Long Short-Term memory," *Neural Computation*, vol. 9, pp. 1735–1780, 11 1997.

[28] F. R. Adaryani, S. J. Mousavi, and F. Jafari, "Short-term rainfall forecasting using machine learning-based approaches of PSO-SVR, LSTM and CNN," *Journal of Hydrology*, vol. 614, p. 128463, 11 2022.

[29] O. Güngör, B. Akşanlı, and R. Aydoğan, "Algorithm selection and combining multiple learners for residential energy prediction," *Future Generation Computer Systems*, vol. 99, pp. 391–400, 10 2019.

[30] R. Garnett, *Bayesian Optimization.* Cambridge University Press, 1 2023.

[31] S. M. Ross, *Introduction to probability and statistics for engineers and scientists.* Academic Press, 8 2014.

[32] P. I. Frazier, "A tutorial on Bayesian optimization," *arXiv (Cornell University)*, 7 2018.

[33] T. Ahmad, H. Chen, Y. Guo, and J. Wang, "A comprehensive overview on the data driven and large scale based approaches for forecasting of building energy demand: A review," *Energy and Buildings*, vol. 165, pp. 301–320, 4 2018.

[34] C. Miller and F. Meggers, "Mining electrical meter data to predict principal building use, performance class, and operations strategy for hundreds of non-residential buildings," *Energy and Buildings*, vol. 156, pp. 360–373, 12 2017.

[35] M. S. Geraldi and E. Ghisi, "Data-driven framework towards realistic bottom-up energy benchmarking using an Artificial Neural Network," *Applied Energy*, vol. 306, p. 117960, 1 2022.

[36] J. Ma and J. Cheng, "Identifying the influential features on the regional energy use intensity of residential buildings based on Random Forests," *Applied Energy*, vol. 183, pp. 193–201, 12 2016.

[37] S. T. Moghadam, J. Toniolo, G. Mutani, and P. Lombardi, "A GIS-statistical approach for assessing built environment energy use at urban scale," *Sustainable Cities and Society*, vol. 37, pp. 70–84, 2 2018.

[38] D. Koschwitz, J. Frisch, and C. Van Treeck, "Data-driven heating and cooling load predictions for non-residential buildings based on support vector machine regression and NARX Recurrent Neural Network: A comparative study on district scale," *Energy*, vol. 165, pp. 134–142, 12 2018.

[39] S. Touzani, J. Granderson, and S. Fernandes, "Gradient boosting machine for modeling the energy consumption of commercial buildings," *Energy and Buildings*, vol. 158, pp. 1533–1543, 1 2018.

[40] M. Kristensen, A. Brun, and S. Petersen, "Predicting Danish residential heating energy use from publicly available building characteristics," *Energy and Buildings*, vol. 173, pp. 28–37, 8 2018.

[41] N. Abbasabadi, M. Ashayeri, R. Azari, B. Stephens, and M. Heidarinejad, "An integrated data-driven framework for urban energy use modeling (UEUM)," *Applied Energy*, vol. 253, p. 113550, 11 2019.

[42] A. A. A. Gassar, G. Y. Yun, and S. Kim, "Data-driven approach to prediction of residential energy consumption at urban scales in London," *Energy*, vol. 187, p. 115973, 11 2019.

[43] W. Wang, T. Hong, X. Xu, J. Chen, Z. Liu, and N. Xu, "Forecasting district-scale energy dynamics through integrating building network and long short-term memory learning algorithm," *Applied Energy*, vol. 248, pp. 217–230, 8 2019.

[44] W. Wang, Q. Lin, J. Chen, X. Li, Y. Sun, and X. Xu, "Urban building energy prediction at neighborhood scale," *Energy and Buildings*, vol. 251, p. 111307, 11 2021.

[45] F. Banihashemi, M. Weber, and W. Lang, "Model order reduction of building energy simulation models using a convolutional neural network autoencoder," *Building and Environment*, vol. 207, p. 108498, 1 2022.

[46] P. Remmen, M. Lauster, M. Mans, M. Fuchs, T. Osterhage, and D. Müller, "TEASER: an open tool for urban energy modelling of building stocks," *Journal of Building Performance Simulation*, vol. 11, pp. 84–98, 2 2017.

[47] J. A. Fonseca, T.-A. Nguyen, A. Schlueter, and F. Maréchal, "City Energy Analyst (CEA): Integrated framework for analysis and optimization of building energy systems in neighborhoods and city districts," *Energy and Buildings*, vol. 113, pp. 202–226, 2 2016.

[48] T. Hong, Y. Chen, S. H. Lee, and M. A. Piette, "Citybes: A web-based platform to support city-scale building energy efficiency," *Urban Computing*, vol. 14, p. 2016, 2016.

[49] M. Österbring, Mata, L. Thuvander, M. Mangold, F. Johnsson, and H. Wallbaum, "A differentiated description of building-stocks for a georeferenced urban bottom-up building-stock model," *Energy and Buildings*, vol. 120, pp. 78–84, 5 2016.

[50] R. Buffat, A. Froemelt, N. Heeren, M. Raubal, and S. Hellweg, "Big data GIS analysis for novel approaches in building stock modelling," *Applied Energy*, vol. 208, pp. 277–290, 12 2017.

[51] Y. Chen, T. Hong, and M. A. Piette, "Automatic generation and simulation of urban building energy models based on city datasets for city-scale building retrofit analysis," *Applied Energy*, vol. 205, pp. 323–335, 11 2017.

[52] J. Schiefelbein, J. Rudnick, A. Scholl, P. Remmen, M. Fuchs, and D. Müller, "Automated urban energy system modeling and thermal building simulation based

on OpenStreetMap data sets," *Building and Environment*, vol. 149, pp. 630–639, 2 2019.

[53] X. Yang, M. Hu, N. Heeren, C. Zhang, T. J. Verhagen, A. Tukker, and B. Steubing, "A combined GIS-archetype approach to model residential space heating energy: A case study for the Netherlands including validation," *Applied Energy*, vol. 280, p. 115953, 12 2020.

[54] S. Bolluk and S. Seyis, *Review of Uncertainties in building Characterization for Urban-Scale Energy Modeling*. 1 2022.

[55] A. A. Famuyibo, A. Duffy, and P. Strachan, "Developing archetypes for domestic dwellings—An Irish case study," *Energy and Buildings*, vol. 50, pp. 150–157, 7 2012.

[56] F. Johari, G. Peronato, P. Sadeghian, X. Zhao, and J. Widén, "Urban building energy modeling: State of the art and future prospects," *Renewable Sustainable Energy Reviews*, vol. 128, p. 109902, 8 2020.

[57] C. Cerezo, J. Sokol, S. AlKhaled, C. Reinhart, A. Al-Mumin, and A. Hajiah, "Comparison of four building archetype characterization methods in urban building energy modeling (UBEM): A residential case study in Kuwait City," *Energy and Buildings*, vol. 154, pp. 321–334, 11 2017.

[58] J. Sokol, C. C. Davila, and C. Reinhart, "Validation of a Bayesian-based method for defining residential archetypes in urban building energy models," *Energy and Buildings*, vol. 134, pp. 11–24, 1 2017.

[59] A. Krayem, A. A. Bitar, A. Ahmad, G. Faour, J.-P. Gastellu-Etchegorry, I. Lakkis, J. A. Gérard, H. Zaraket, A. Yeretzian, and S. Najem, "Urban energy modeling and calibration of a coastal Mediterranean city: The case of Beirut," *Energy and Buildings*, vol. 199, pp. 223–234, 9 2019.

[60] C.-K. Wang, S. H. Tindemans, C. Miller, G. Agugiaro, and J. Stoter, "Bayesian calibration at the urban scale: a case study on a large residential heating demand application in Amsterdam," *Journal of Building Performance Simulation*, vol. 13, pp. 347–361, 2 2020.

[61] M. Gholami, D. Torreggiani, P. Tassinari, and A. Barbaresi, "Narrowing uncertainties in forecasting urban building energy demand through an optimal archetyping method," *Renewable Sustainable Energy Reviews*, vol. 148, p. 111312, 9 2021.

[62] S. S. Abolhassani, M. Amayri, N. Bouguila, and U. Eicker, "A new workflow for detailed urban scale building energy modeling using spatial joining of attributes for archetype selection," *Journal of Building Engineering*, vol. 46, p. 103661, 4 2022.

[63] M. Kristensen, R. E. Hedegaard, and S. Petersen, "Long-term forecasting of hourly district heating loads in urban areas using hierarchical archetype modeling," *Energy*, vol. 201, p. 117687, 6 2020.

[64] M. Kristensen, R. E. Hedegaard, and S. Petersen, "Hierarchical calibration of archetypes for urban building energy modeling," *Energy and Buildings*, vol. 175, pp. 219–234, 9 2018.

[65] R. E. Hedegaard, M. Kristensen, T. H. Pedersen, A. Brun, and S. Petersen, "Bottom-up modelling methodology for urban-scale analysis of residential space heating demand response," *Applied Energy*, vol. 242, pp. 181–204, 5 2019.

[66] S. Nagpal and C. Reinhart, "A comparison of two modeling approaches for establishing and implementing energy use reduction targets for a university campus," *Energy and Buildings*, vol. 173, pp. 103–116, 8 2018.

[67] P. J. Nageler, A. Koch, F. Mauthner, I. Leusbrock, T. Mach, C. Hochenauer, and R. Heimrath, "Comparison of dynamic urban building energy models (UBEM): Sigmoid energy signature and physical modelling approach," *Energy and Buildings*, vol. 179, pp. 333–343, 11 2018.

[68] S. T. Moghadam, S. Coccolo, G. Mutani, P. Lombardi, J.-l. Scartezzini, and D. Mauree, "A new clustering and visualization method to evaluate urban heat energy planning scenarios," *Cities*, vol. 88, pp. 19–36, 5 2019.

[69] R. Nouvel, A. Mastrucci, U. Leopold, O. Baume, V. Coors, and U. Eicker, "Combining GIS-based statistical and engineering urban heat consumption models: Towards a new framework for multi-scale policy support," *Energy and Buildings*, vol. 107, pp. 204–212, 11 2015.

[70] M. Braulio-Gonzalo, J. P. Paz, M. D. Bovea, and M. J. R. Aguilar, "Modelling energy efficiency performance of residential building stocks based on Bayesian statistical inference," *Environmental Modelling and Software*, vol. 83, pp. 198–211, 9 2016.

[71] A. Nutkiewicz, Z. Yang, and R. K. Jain, "Data-driven Urban Energy Simulation (DUE-S): A framework for integrating engineering simulation and machine learning methods in a multi-scale urban energy modeling workflow," *Applied Energy*, vol. 225, pp. 1176–1189, 9 2018.

[72] O. Pasichnyi, J. Wallin, and O. Kordas, "Data-driven building archetypes for urban building energy modelling," *Energy*, vol. 181, pp. 360–377, 8 2019.

[73] M. Deru, K. Field, D. Studer, K. Benne, B. Griffith, P. Torcellini, B. Liu, M. A. Halverson, D. Winiarski, M. Rosenberg, M. Yazdanian, J. Huang, and D. B. Crawley, "U.S. Department of Energy Commercial Reference Building Models of the National Building Stock," tech. rep., 2 2011.

[74] Y. Q. Ang, Z. Berzolla, S. Letellier-Duchesne, V. Jusiega, and C. Reinhart, "UBEM.io: A web-based framework to rapidly generate urban building energy models for carbon reduction technology pathways," *Sustainable Cities and Society*, vol. 77, p. 103534, 2 2022.

[75] C. Reinhart, T. Dogan, A. Jakubiec, T. Rakha, and A. Sang, "UMI – an urban simulation environment for building energy use, daylighting and walkability," *Building Simulation Conference proceedings*, 8 2013.

[76] U. E. P. Agency and U. D. of Energy, "ENERGY STAR Score for Swimming Pools," 2023.

[77] S. Murakawa, D. Nishina, H. Takata, and A. Tanaka, "An analysis on the loads of hot water consumption in the restaurants," 2005.

[78] L. Pérez-Lombard, J. Ortiz, and C. Pout, "A review on buildings energy consumption information," *Energy and Buildings*, vol. 40, pp. 394–398, 1 2008.

[79] E. Fuentes, L. Arce, and J. Salom, "A review of domestic hot water consumption profiles for application in systems and buildings energy performance analysis," *Renewable Sustainable Energy Reviews*, vol. 81, pp. 1530–1547, 1 2018.

[80] F. D. Salim, B. Dong, M. Ouf, Q. Wang, I. Pigliautile, X. Kang, T. Hong, W. Wu, Y. Liu, S. K. Rumi, M. S. Rahaman, J. An, H. Deng, W. Shao, J. Dziedzic, F. C. Sangogboye, M. B. Kjærgaard, M. Kong, C. Fabiani, A. L. Pisello, and D. Yan, "Modelling urban-scale occupant behaviour, mobility, and energy in buildings: A survey," *Building and Environment*, vol. 183, p. 106964, 10 2020.

[81] S. Shalev-Shwartz and S. Ben-David, *Understanding machine learning.* 5 2014.

VITA

Said Bolluk received his undergraduate degree from the Department of Civil Engineering at Özyeğin University in 2019. He has been resuming his master's education in Civil Engineering since 2021 while working as a teaching assistant at Özyeğin University. He also works as a researcher within the scope of a TÜBİTAK project. His research interests include improving urban planning strategies through machine learning.

PUBLICATIONS

- Bolluk, S., Seyis, S., & Aydoğan, R. (2023). Feature extraction for enhancing data-driven urban building energy models. Computing in Construction. `https://doi.org/10.35490/ec3.2023.291`

- Bolluk, S., & Seyis, S. (2022). Review of Uncertainties in building Characterization for Urban-Scale Energy Modeling. In Springer eBooks (pp. 159–182). `https://doi.org/10.1007/978-3-031-16895-6_11`

- Bolluk, S., & Seyis, S. (2022). Handling Imbalanced Data in Building Energy Benchmarking. In The 7th International Project and Construction Management Conference (IPCMC2022). `https://www.researchgate.net/publication/365730308_Handling_Imbalanced_Data_in_Building_Energy_Benchmarking`